

**Monte Carlo Model for Designing  
Fluorescent Materials in a Spectral Filter**

by

Justin D. Ging

Submitted to the Electrical Engineering and Computer Science  
in Partial Fulfillment of the Requirements for the Degree of  
Master of Engineering in Electrical Engineering and Computer Science  
at the Massachusetts Institute of Technology

May 21, 1999

© Copyright 1999 Justin D. Ging. All rights reserved.

The author hereby grants to M.I.T. permission to reproduce and  
distribute publicly paper and electronic copies of this thesis  
and to grant others the right to do so.

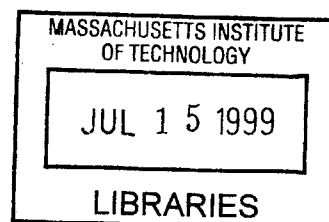
Author \_\_\_\_\_  
Department of Electrical Engineering and Computer Science  
May 14, 1999

Certified by \_\_\_\_\_  
Cardinal Warde  
M.I.T. Thesis Supervisor

Certified by \_\_\_\_\_  
David M. Reilly  
VI-A Company Thesis Supervisor

Accepted by \_\_\_\_\_  
Arthur C. Smith  
Chairman, Department Committee on Graduate Theses

ENG



Monte Carlo Model for Designing  
Fluorescent Materials in a Spectral Filter

by  
Justin D. Ging

Submitted to the  
Department of Electrical Engineering and Computer Science

May 14, 1999

In Partial Fulfillment of the Requirements for the Degree of  
Master of Engineering in Electrical Engineering and Computer Science

## **ABSTRACT**

A Monte Carlo simulation model capable of predicting fluorescence behavior of an illuminated spectral filter material in a photon counting regime is presented. The model accepts input data for a source, input filter, fluorescing material, output filter and detector. Fluorescing materials are described by excitation and emission data, which can be data measured from a real material or just an analytical shape. The user can adjust a variety of input parameters, including the side boundary conditions, input angle, the diameter of the input beam, the length/diameter ratio, and the configuration of the detector. The effects of changing these parameters are presented in terms of meeting goals to either maximize or minimize the fluorescence which reaches the detector. Design problems which recommend a process for selecting parameters are included. Suggestions for improving the usefulness of the model as a tool for the optical designer are given.

M.I.T. Thesis Supervisor: Cardinal Warde  
Title: Professor, MIT

VI-A Company Thesis Supervisor: David Reilly  
Title: Senior Engineering Fellow, Lockheed Martin IR Imaging Systems

To my parents, whose love and support made this possible.

## Acknowledgments

I am deeply grateful to my mentor, Mr. David Reilly. He not only provided a tremendous amount of guidance and support, but also shared with me his wisdom and vision on subjects ranging far beyond the scope of this thesis. I hope that someday I might offer even half as much help to someone as he gave me.

Professor Warde was kind enough to take me on as an advisee. His questions and suggestions added focus and substance to my work. I appreciate the time and attention he offered.

I thank Mr. Warren Clark for his effective analysis of the results of my model. He spent many hours with me looking for, and solving a critical bug. His insights and explanations were essential to my understanding of interactions in my model.

Lockheed Martin graciously provided me with the facilities and knowledgeable employees to assist me throughout my endeavor. I would like to thank Mr. Burton Figler for his supervision and administrative guidance, Mr. Peter Campoli for his support and funding, and Mr. Bruce Baran for his interest and encouragement.

Mr. Steven Duclos, of GE Corporate Research & Development, cheerfully offered his expertise on fluorescence and luminescence.

I thank my friends, Chad Talbott and Amy Yen, for their assistance. Chad provided algorithms and advice for improving my code and Amy tirelessly proofread my thesis. Their support was invaluable.

My parents provided love, encouragement, and financial support, for which I am fortunate. They listened patiently to my often cryptic explanations of the Monte Carlo process, and counseled me through mental dry spells.



# Table of Contents

<i>Title Page</i>	1
<i>Abstract</i>	2
<i>Dedication</i>	3
<i>Acknowledgments</i>	4
<i>Table of Contents</i>	5
<i>List of Figures</i>	7
<i>List of Tables</i>	8
<u><i>1.0 Introduction</i></u>	9
<i>1.1 Remote Sensing</i>	11
<i>1.2 Photon Counting</i>	12
<i>1.3 Spectral Filtering</i>	13
<u><i>2.0 Fluorescence</i></u>	14
<i>2.1 Fluorescence/Photoluminescence</i>	15
<i>2.2 Measuring Fluorescence</i>	17
<u><i>3.0 Monte Carlo Simulation Model</i></u>	21
<i>3.10 Model</i>	22
<i>3.11 Source</i>	23
<i>3.12 Input Filter</i>	23
<i>3.13 Fluorescing Element</i>	23
<i>3.14 Output Filter</i>	24
<i>3.15 Detector</i>	24
<i>3.20 Monte Carlo Process</i>	25
<i>3.30 Statistical Methods</i>	29
<i>3.31 Initial Position</i>	30
<i>3.32 Initial Wavelength</i>	31
<i>3.33 Initial Direction</i>	32
<i>3.34 Distance to Absorption Point</i>	33
<i>3.35 Re-radiation Direction</i>	33
<i>3.36 Re-radiation Wavelength</i>	34
<i>3.40 Data Output</i>	35
<i>3.41 Spectral Data</i>	35
<i>3.42 Angular Data</i>	36
<i>3.43 Positional Data</i>	36
<i>3.44 Trapped Photons</i>	37
<u><i>4.0 Model Parameter Effects</i></u>	39
<i>4.1 Spectral Characteristics of Material</i>	41
<i>4.2 Boundary Effects</i>	48
<i>4.3 Input Angle</i>	54
<i>4.4 Diameter of Input</i>	61

<i>4.5 Length/Diameter Ratio (<math>\alpha l</math> constant)</i>	67
<i>4.6 Detector Configuration</i>	72
<u><i>5.0 Design Configurations</i></u>	78
<i>5.1 Maximize Fluorescence</i>	80
<i>5.2 Minimize Fluorescence</i>	81
<u><i>6.0 Conclusion/Recommendations</i></u>	82
<i>Appendix A – Flowchart of Monte Carlo Simulation</i>	84
<i>References</i>	88

## List Of Figures

Figure 1- Fluorescing materials in the spectral filter of a photon counting sensor.....	9
Figure 2- Remote Sensing.....	11
Figure 3- Photon Counting Sensor.....	12
Figure 4- Interactions Between Light and Matter.....	13
Figure 5- Schematic Diagram of Photoluminescence.....	14
Figure 6- Spectrofluorometer Configurations.....	18
Figure 7- Excitation and Emission Spectra of Fluorescent Glasses.....	19
Figure 8- Monte Carlo Model Components.....	22
Figure 9- Specifications of Material Properties.....	24
Figure 10- Monte Carlo Simulation Possibilities.....	25
Figure 11- Schematic of Boundary Interaction.....	26
Figure 12- Deciding if a Photon is Absorbed in the Material.....	27
Figure 13- Choosing a Random Start Location.....	30
Figure 14- Cumulative Density Function (CDF).....	31
Figure 15- Calculating Initial Direction.....	32
Figure 16- Calculating the Distance a Photon Travels.....	33
Figure 17- Trapping Geometries.....	38
Figure 18- Total Internal Reflection (TIR) Preventing Transmission.....	38
Figure 19- Gaussian Distribution.....	40
Figure 20- Excitation and Emission Spectra Configurations.....	41
Figure 21- Emission for Separated Spectra.....	43
Figure 22- Emission for Overlapping Spectra.....	45
Figure 23- Side Boundary Configurations.....	48
Figure 24- Angular Distribution of Fluorescent Photons.....	52
Figure 25- Input Angle Configuration.....	54
Figure 26- Direct Photons vs. Input Angle for Various Side Boundaries.....	56
Figure 27- Angular Distribution for Two Input Angles (Air).....	58
Figure 28- Angular Distribution for Two Input Angles (Diffuse Reflective).....	59
Figure 29- Input Beam Diameter Configuration.....	61
Figure 30- Fluorescent Photon Spatial Distribution for Various Input Diameters.....	64
Figure 31- Fluorescent Photon Angular Distribution for Various Input Diameters.....	65
Figure 32- Length/Diameter Ratio Configuration.....	67
Figure 33- Fluorescent Photons vs. Length/Diameter Ratio.....	69
Figure 34- Fluorescent Photon Angular Distributions for Length/Diameter Ratios.....	70
Figure 35- Detector Configuration.....	72
Figure 36- Fluorescent Photons vs. Length for Coupled and Uncoupled Detectors.....	75
Figure 37- Fluorescent Photon Angular Distribution for Various Lengths.....	76
Figure 38- Parameter Selection Procedure.....	79

## List Of Tables

<i>Table 1- Optical Properties of Fluorescent Glasses</i> .....	20
<i>Table 2- Possible Photon Destinations</i> .....	35
<i>Table 3- Configurations Considered</i> .....	39
<i>Table 4- Spectral Characteristics Test Cases</i> .....	42
<i>Table 5- Monte Carlo Test Results for Separated Spectra</i> .....	46
<i>Table 6- Monte Carlo Test Results for Overlapping Spectra</i> .....	46
<i>Table 7- Parameter Choices for Each Goal</i> .....	47
<i>Table 8- Boundary Effects Test Cases</i> .....	49
<i>Table 9- Monte Carlo Test Results for Cladded Side Boundary</i> .....	50
<i>Table 10- Monte Carlo Test Results for Air Side Boundary</i> .....	50
<i>Table 11- Monte Carlo Test Results for Diffuse Reflective Boundary</i> .....	51
<i>Table 12- Parameter Choices for Each Goal</i> .....	53
<i>Table 13- Input Angle Test Cases</i> .....	55
<i>Table 14- Parameter Choice for Each Goal</i> .....	60
<i>Table 15- Input Diameter Test Cases</i> .....	62
<i>Table 16- Monte Carlo Test Results for Beam Input</i> .....	63
<i>Table 17- Monte Carlo Test Results for Spot Input</i> .....	63
<i>Table 18- Monte Carlo Test Results for Flooded Input</i> .....	63
<i>Table 19- Parameter Choice for Each Goal</i> .....	66
<i>Table 20- Length/Diameter Ratio Test Cases</i> .....	68
<i>Table 21- Parameter Choice for Each Goal</i> .....	71
<i>Table 22- Detector Configuration Cases</i> .....	73
<i>Table 23- Monte Carlo Test Results for Optically Coupled Detector</i> .....	74
<i>Table 24- Monte Carlo Test Results for Uncoupled Detector</i> .....	74
<i>Table 25- Parameter Choice for Each Goal</i> .....	77
<i>Table 26- Parameter Choices for Each Goal</i> .....	79

## 1.0 Introduction

The goal of photon counting is to optimally detect desired signal(s) in the presence of competing sources. A photon counting sensor employs a spectral filter to discriminate among a variety of signals and to shape the signal which reaches the detector. Certain materials comprising the spectral filter may fluoresce, allowing the filter to operate in one of two possible modes. This arrangement is shown in Figure 1.

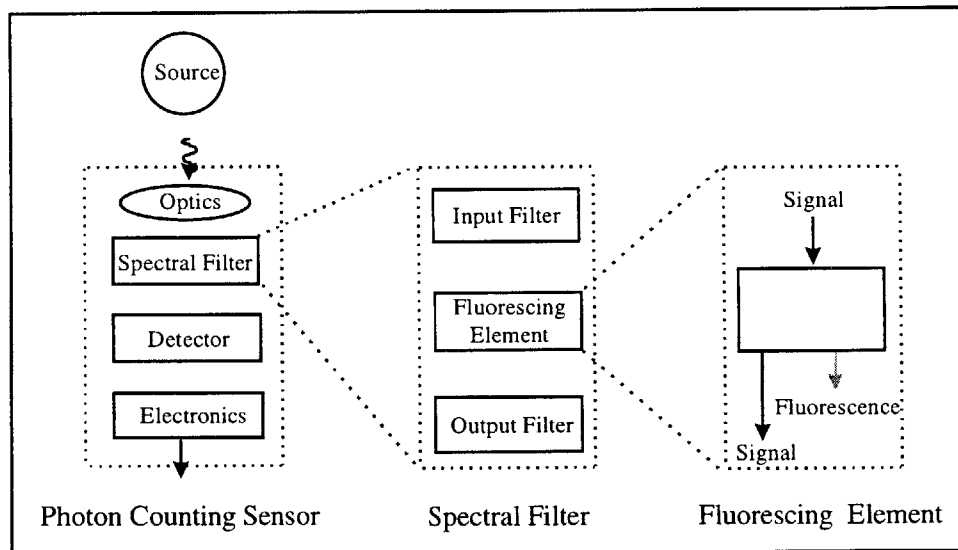


**Figure 1- Fluorescing materials in the spectral filter of a photon counting sensor.**

If the fluorescence results from out-of-band signal excitation, then the fluorescence can be considered as a dependent noise source. In this case, the filter would operate in a fluorescence rejection mode, whereby attempts would be made to reduce the excitation and emission of the fluorescence as well as configure the fluorescing element to minimize fluorescent events. On the other hand, if the fluorescence in the spectral filter results from the in-band, desired signal, attempts would be made to enhance the fluorescence. In some

cases, the wavelength shifting property of fluorescence might be utilized to take advantage of available detectors. For either of the two modes of operation, it is necessary to understand the parameters which determine the fluorescence characteristics of a material used in a spectral filter.

For this thesis, I have created a model which predicts the behavior of fluorescence in a spectral filter. The model is a Monte Carlo simulation which uses non-sequential ray tracing to track individual photons through a virtual fluorescent material. The destination of each photon is dependent upon a series of probability laws.

In the first two sections, I introduce fluorescence and its relationship to the spectral filter. I discuss applications of fluorescence and techniques for measuring fluorescence. In Section 3, I describe the Monte Carlo model's form and function, as well as the types of data which the model produces. Section 4 focuses on six categories of input parameters to the model, each of which can be adjusted to either maximize or minimize fluorescence. I use the general concepts developed in this section to solve specific design examples in Section 5. One problem seeks to maximize fluorescence, the other to minimize. Finally, in Section 6, I discuss further improvements which could be made to the model to increase its utility for an optical designer.

## 1.1 Remote Sensing

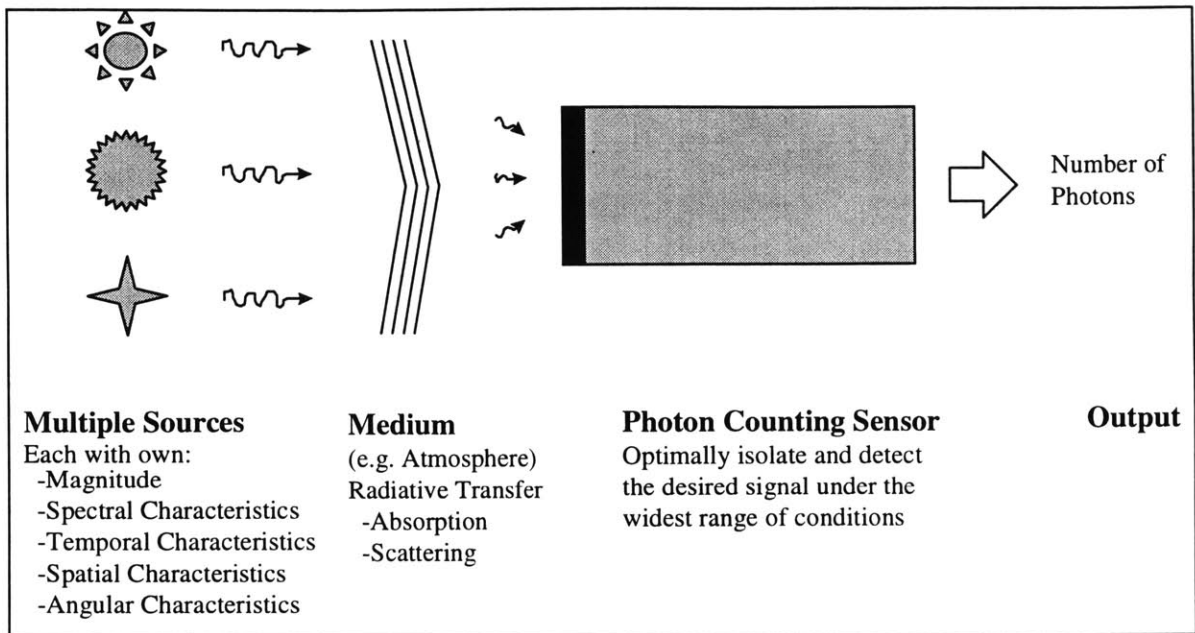


**Figure 2- Remote Sensing**

A remote sensing problem, as illustrated in Figure 2, may involve many different sources contributing to the radiation incident on a photon counting sensor. Each of the multiple sources has its own magnitude, as well as spectral, angular, temporal and spatial characteristics. As radiation from these sources travels through the medium, its characteristics are modified as a result of absorption and scattering interactions<sup>1,2</sup>. When the resultant light reaches the sensor, the sensor must isolate and detect the desired information over a wide dynamic range. Finally, the sensor outputs a number of photons.

## 1.2 Photon Counting

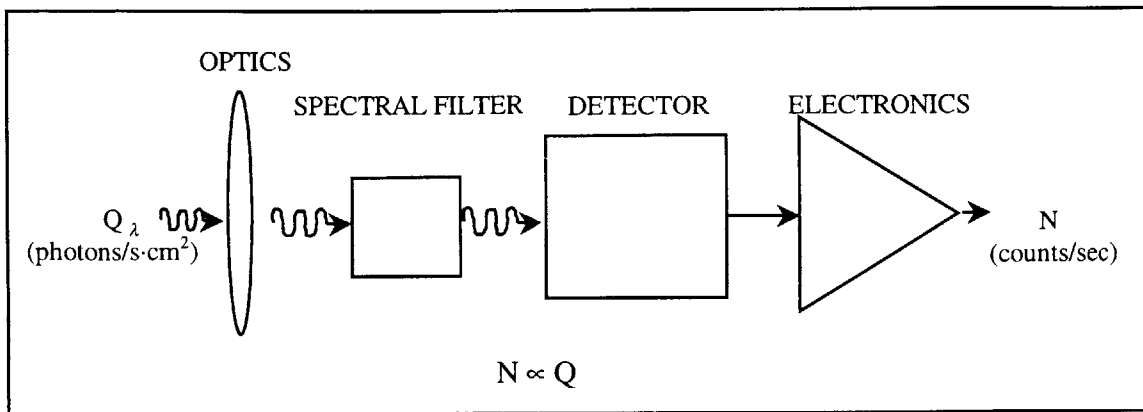


**Figure 3- Photon Counting Sensor**

Photon counting sensors make it possible to accurately detect low-level signals<sup>3,4</sup>. They provide a numerical output which is proportional to the photon flux incident on the sensor. The photon counting sensor is comprised of optics, a spectral filter, a detector, and electronics<sup>5</sup>, as shown in Figure 3. The optics collect and focus the light impinging on the front surface of the sensor<sup>6</sup>. The spectral filter isolates the desired wavelength(s) from competing radiation. The detector converts the optical signal to an electronic signal<sup>7</sup>. Finally, the electronics amplify and shape the signal and present it at the output.



## 1.3 Spectral Filtering

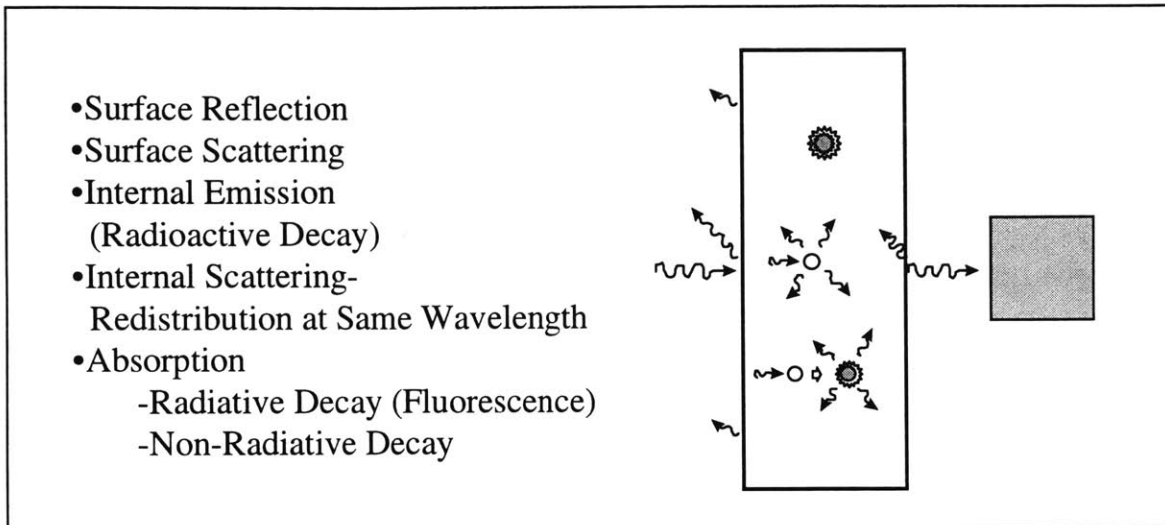


**Figure 4- Interactions Between Light and Matter**

The spectral filter may include several different materials and utilize various filtering techniques. This thesis will be primarily concerned with spectral filters based on absorbing materials. As the light passes through the spectral filter, there are many possible interactions between the radiation and filter elements<sup>8</sup>. These interactions, shown in Figure 4, include surface reflection, surface and bulk scattering, absorption, and self-emission<sup>9</sup>. Scattering interactions result in spatial redistribution at the same wavelength. Absorbing interactions result in either a total loss of energy or a radiative decay. If the radiative decay occurs in a short enough (10ns) time scale, it is called fluorescence.

## 2.0 Fluorescence

Fluorescence is part of a larger classification called luminescence. Luminescence is optical radiation caused by an applied external source of energy. There are many ways in which a material may be caused to luminesce. For example, great pressure or shaking may cause triboluminescence where luminescence results from sparks emanating from microfissures in the material<sup>10,11</sup>. Other examples include chemiluminescence, cathodoluminescence, bioluminescence, and sonoluminescence, which are caused by chemical reactions, collisions of accelerated electrons, living organisms, and energy from a sound wave, respectively. The luminescence of interest in this thesis is that which is caused by photoexcitation, called photoluminescence. At the quantum level, photoluminescence occurs when a photon impacts an atom, exciting it and causing it to promote an electron to a higher energy level. When the electron decays to a lower energy level, the atom re-radiates a photon of less energy than the impacting photon and thus of a longer wavelength. When the decay process occurs within 10ns, the photoluminescence is classified as fluorescence<sup>12,13</sup>. The quantum process is illustrated in Figure 5.

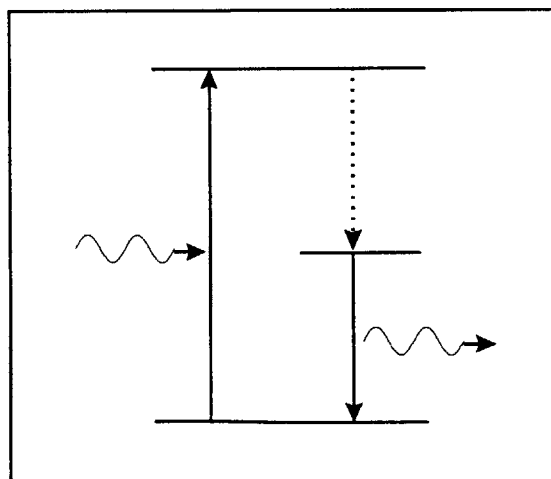


**Figure 5- Schematic Diagram of Photoluminescence**

## 2.1 Fluorescence Applications

People come into contact with fluorescence phenomena every day, yet many are not aware of the degree to which fluorescence, in its many and varied forms, pervades society. Fluorescence can be found around the home in lighting, bright-whitening laundry detergent, and highlighting markers. It can be found on farms, detecting the health of plants<sup>14</sup>, in doctor's offices, eliminating the need for needle sticks<sup>15</sup>, and in researcher's labs, distinguishing between live and dead bacteria<sup>16</sup>. Marine biologists are using fluorescence to determine reef health<sup>17</sup> while preservationists are analyzing historic facades<sup>18</sup>. Environmentalists use fluorescence to sense oil films on natural waters<sup>19</sup> and to monitor atmospheric pollutants which contribute to acid rain<sup>20</sup>. Engineers are utilizing fluorescence to develop electronic x-ray detectors<sup>21</sup>, eliminating the need for film. People are surrounded by fluorescence.

Applications of fluorescence provide illustrations of the fluorescence process. The most familiar application of fluorescence may be fluorescent lighting used in places such as homes, offices, and stores<sup>22</sup>. A fluorescent light bulb is composed of a glass tube with metal electrodes sealed into its ends. The tube contains some gas such as argon along with a small amount of mercury. When the bulb is turned on, the electrodes ionize the mercury atoms which then discharge and create a line emission at 254nm. A phosphor coating on the inside of the glass tube is excited by the emission at 254nm and emits, or fluoresces, at visible wavelengths which make up the "white" appearance of the light.

In essence, the operation of the phosphor is an up-conversion in wavelength (down-conversion in energy) in that it converts ultraviolet (UV) wavelengths of light into visible wavelengths of light. Phosphors which perform up-conversion are referred to as

wavelength shifters, or scintillators. Phosphors are not limited to up-conversion of only UV, but instead can be used to up-convert x-rays to visible light. X-ray scintillators are being employed in devices which may obviate the need for medical x-ray films, and will provide instant x-ray results<sup>21</sup>. X-rays are passed through a person, for example, impinge upon the scintillating phosphor and are converted to visible light wavelengths. The photons may then be recorded by an electronic detector such as a CCD. Electronic detectors are being developed for UV and x-ray wavelengths, but cost, availability, and other factors, make the scintillator/CCD combination more desirable.

## 2.2 Measuring Fluorescence

The most salient properties of a fluorescent material are its excitation and emission spectra. The excitation spectrum describes the relative emission intensity observed from a fluorescing molecule at a single wavelength for a range of wavelengths exciting the molecule. The emission spectrum describes the relative intensity of emission observed over a range of wavelengths, for a fixed excitation wavelength. These spectra are unique to each molecule and thus are useful qualitative data. It is possible for a material to have multiple types of fluorescing molecules, resulting in excitation and emission spectra which are superpositions of the spectra for each type of molecule. Often, biological samples, such as corals, are multi-pigmented and have complex spectra<sup>23</sup>.

Several methods are available for measuring the fluorescence properties of materials. The method chosen is dependent on which fluorescence characteristics one wishes to measure. Another fluorescence property, besides emission and excitation, which can be measured is the “lifetime”, or period of decay, of a fluorescent event for a given set of excitation conditions.

One method used to measure a molecule’s characteristic excitation and emission spectra is spectrofluorimetry. A spectrofluorometer is comprised of a source, input monochromator, sample chamber, output monochromator, and detector. The geometry of the setup depends on the sample being measured. Two possible geometries are shown in Figure 6. For a liquid sample in a cuvet, a perpendicular geometry would be chosen, such that the emission would be viewed at 90° from the excitation. This would maximize the fluorescence collected and minimize the amount of scattered excitation light. For a solid

sample, a reflectance geometry would be employed, whereby the emission would be viewed off the front of the sample but not at the angle of the reflected excitation.

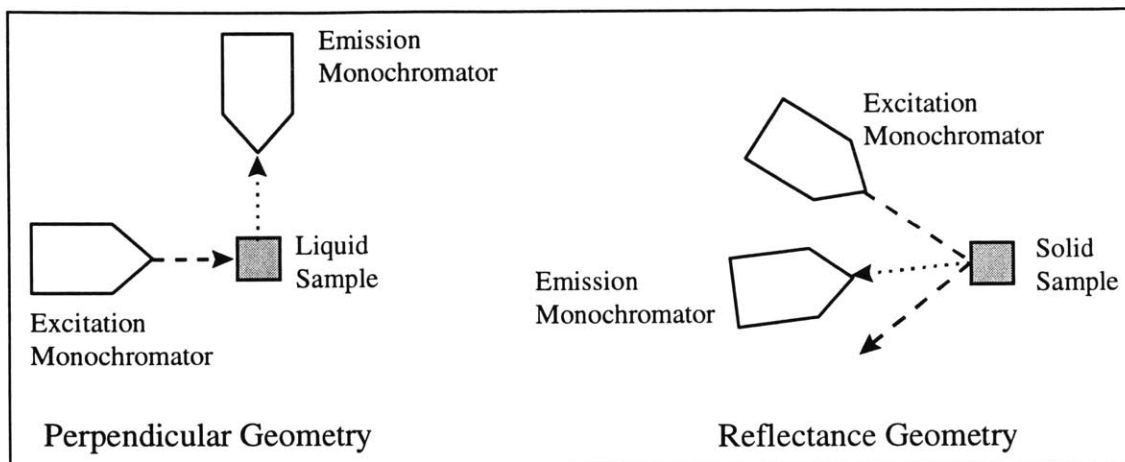


**Figure 6- Spectrofluorometer Configurations**

The Spectrofluorimetry process begins by selecting an excitation wavelength. With the excitation monochromator fixed at the selected wavelength, the emission monochromator is scanned over a range of wavelengths. The resulting emission spectrum is analyzed in search of peaks. A wavelength at which a large peak occurs is chosen and used to set the emission monochromator. The excitation monochromator is then scanned over a range of wavelengths while the emission monochromator is held fixed. In this iterative process, excitation and emission spectra are determined which display intensities for wavelength regions where fluorescence efficiency is greatest.

Other methods for determining a molecule's characteristic excitation and emission spectra are variations of spectrofluorimetry which use different types of sources to excite the molecule. Another source could be photons of twice the excitation wavelength, such that fluorescence only occurs when two photons impact a molecule at the same time, and

thus provide sufficient energy to excite its atoms. Still another source might be x-ray radiation.

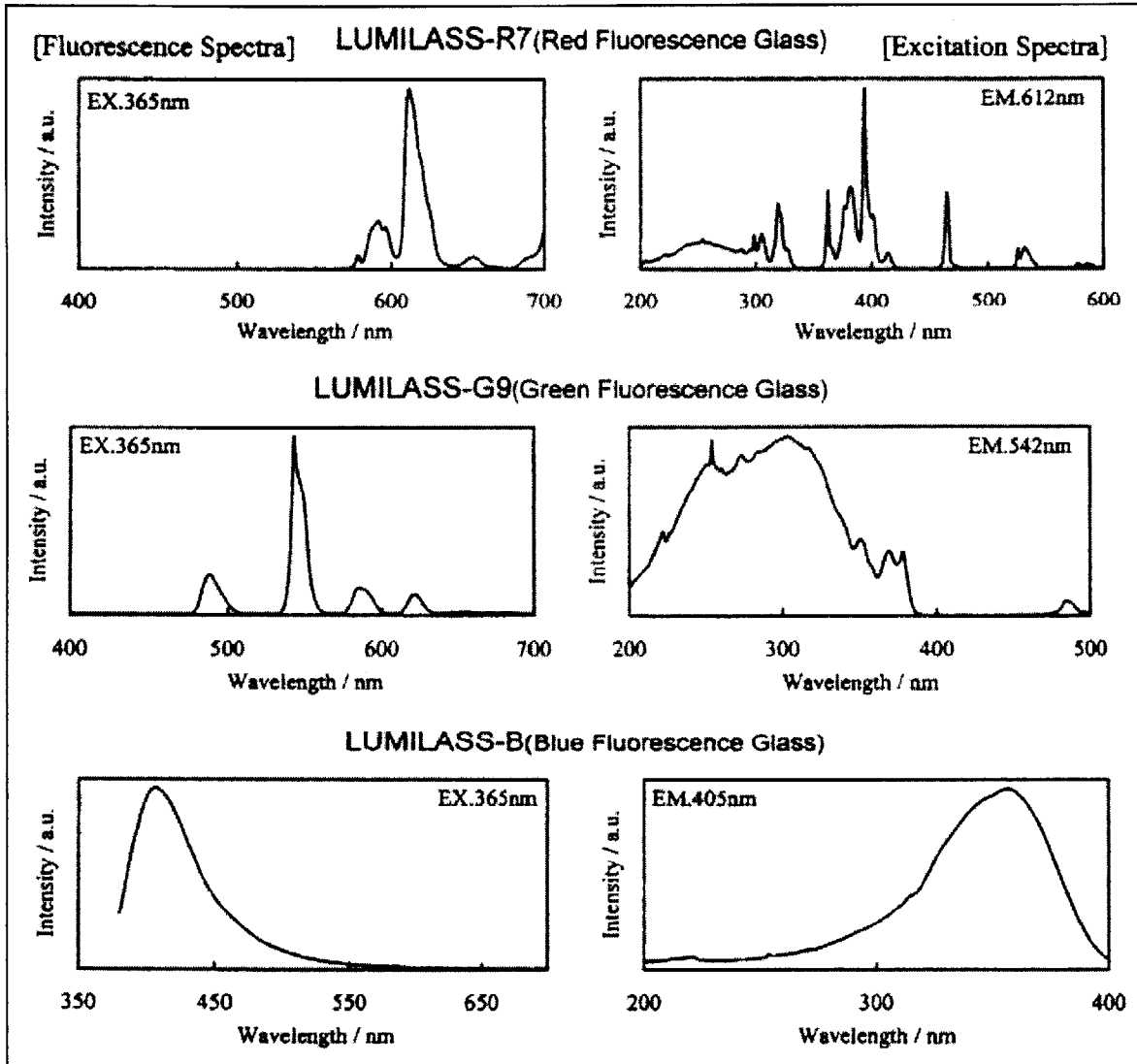


Figure 7- Excitation and Emission Spectra of Fluorescent Glasses made by Sumita Optical Glass

Figure 7 shows spectra examples of real fluorescent materials made by Sumita Optical Glass<sup>24</sup>. Sumita provides emission and excitation spectra to characterize their fluorescent glasses, as well as some optical properties of the glass, listed in Table 1. Most likely, these data were acquired by spectrofluorimetry. By looking at the data, one might notice that the green fluorescent glass would have good potential for use as a wavelength

shifter because of the separation between the emission spectra and the wavelength range covered by the excitation spectrum.

Optical Properties			
	LUMILASS-R7	LUMILASS-G9	LUMILASS-B
Main Fluorescence Wavelength (nm)	610	540	405
Excitation Wavelength Range (nm)	200-420	200-390	200-400
Minimum Sensitivity ( $\mu$ W/cm <sup>2</sup> )	<1	<1	<1
Refractive Index (nd)	1.645	1.694	1.477

Thermal and Mechanical Properties			
	LUMILASS-R7	LUMILASS-G9	LUMILASS-B
Transformation Point(°C)	594	660	398
Thermal Expansion (1/°C)	$86 \times 10^{-7}$	$73 \times 10^{-7}$	$176 \times 10^{-7}$
Specific Gravity (g/cm <sup>3</sup> )	3.77	3.76	3.65
Vickers Hardness (Kg/mm <sup>2</sup> )	633	765	344
Young's Modulus ( $\times 10^9$ Pa)	90	114	65
Modulus of Rigidity ( $\times 10^9$ Pa)	34	44	25

Table 1- Optical Properties of Fluorescent Glasses

Fluorescence Lifetime Spectrometry is the method used to measure fluorescence decay. Setup for such a technique is similar to a spectrofluorometer except that the source used is pulsed and collection of the emitted signal is accomplished by a multichannel analyzer. The times required for pulses to reach the analyzer are summed into a histogram whose slope indicates the characteristics of the fluorescence decay<sup>25</sup>.

Measurement of fluorescence in a transmission geometry is difficult to achieve since the source radiation is many orders of magnitude more intense than the fluorescence. Furthermore, because of the complexity of fluorescent events, analytic methods to determine expected fluorescence output are overwhelming. Thus a simulation modeling technique offers a manageable way to determine fluorescence in a transmission geometry.



### 3.0 Monte Carlo Simulation Model

Ideally, a model is based solely on analytical equations which describe the phenomenon. However, when analytical equations become too complex or do not exist, one must call on other modeling techniques. One such useful method is the Monte Carlo (MC) method<sup>26,27</sup>. For optical applications, the MC method tracks individual photons through a material. Many possible interactions can be accounted for using probability laws to decide if things such as absorption events or reflections occur<sup>28,29</sup>.

The MC simulation model presented here includes fluorescence and therefore utilizes non-sequential ray tracing. The destiny of a photon is not known a priori requiring that the photon be tracked as it progresses through the fluorescing element. It is intended that the MC simulation could be included in a larger ray tracing or optical design program by making some adjustments to accommodate specific input and output criteria.

### 3.10 Monte Carlo Model

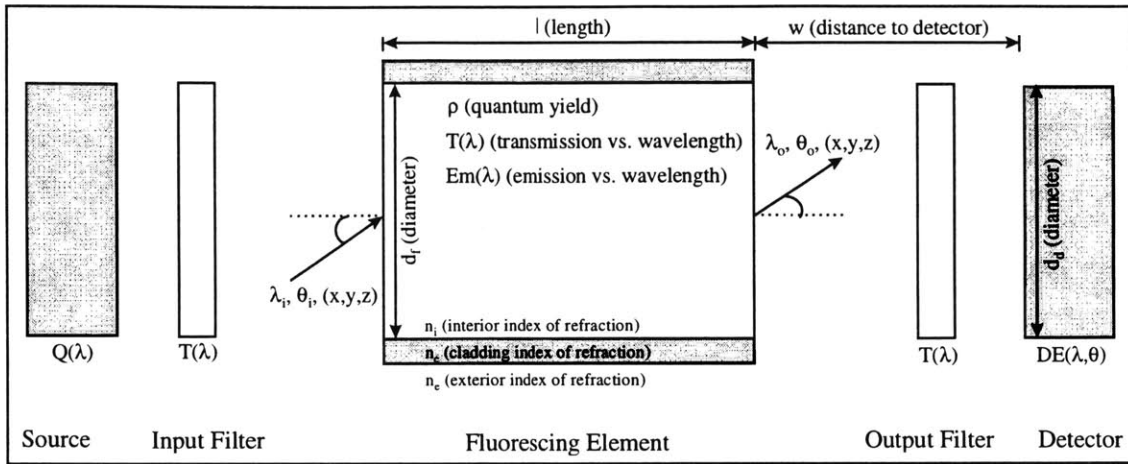


**Figure 8- Monte Carlo Model Components**

The model is composed of five main parts, illustrated in Figure 8. The first part of the model, the source, represents all of the competing signals in the environment of the sensor. The remaining four parts make up the sensor itself. The input filter does some preliminary shaping of signals in the environment before they enter the fluorescing element. The fluorescing element is the core of the sensor model. It, too, shapes the input signal but, in addition, produces a fluorescent signal. The output from the fluorescing element leads into the output filter which separates the desired signal from the fluorescence. Finally, the detector collects the resulting signal.

The following sections describe the data which specify the material properties for each component of the model. Figure 9 summarizes these inputs.

### 3.11 Source

In the MC model, the source is described by an intensity versus wavelength spectrum at a 1nm resolution. The spectrum is the superposition of all the signals in the environment of the sensor. Usually signals must travel through a medium to reach the sensor and are modified by that medium according to some transfer function. The intensity data describing the source include the modifications by the medium.

### 3.12 Input Filter

The input filter is described in the MC model by transmission versus wavelength data at a 1nm resolution. This filter can be used to control the excitation of the fluorescing element which follows it. Often, the filter is a bandpass type. It is assumed that this filter is very thin and thus does not significantly refract incident light rays.

### 3.13 Fluorescing Element

The fluorescing element is assumed to be a homogeneous doped material. For the MC model it is a cylindrical shape with variable radius and length. The walls of the cylinder are surrounded by air, a cladding, or some other material. The indices of refraction for the element, its cladding and the surrounding medium are specified by the user of the model. The optical properties of the crystal material are characterized by transmission data and emission data, both with respect to wavelength. The transmission is used to find the absorbance of the material which is assumed to be spectrally the same as

the material's excitation characteristics. The emission data is used to describe the wavelengths at which atoms in the material re-radiate.

### 3.14 Output Filter

The output filter is similar to the input filter except that it selects out a different range of wavelengths. Like the input filter, it is described by transmission versus wavelength data and is assumed to be very thin so that refraction can be neglected.

### 3.15 Detector

The detector is characterized by detector efficiency (DE) data. DE is dependent on both the angle of incidence upon the detector and the wavelength of the impinging light rays. The user may vary the diameter of the detector to achieve either fluorescence enhancement or rejection. The user may also assign an index of refraction to the detector, so that optical coupling may be implemented. The output from the detector consists of an intensity versus wavelength spectrum.

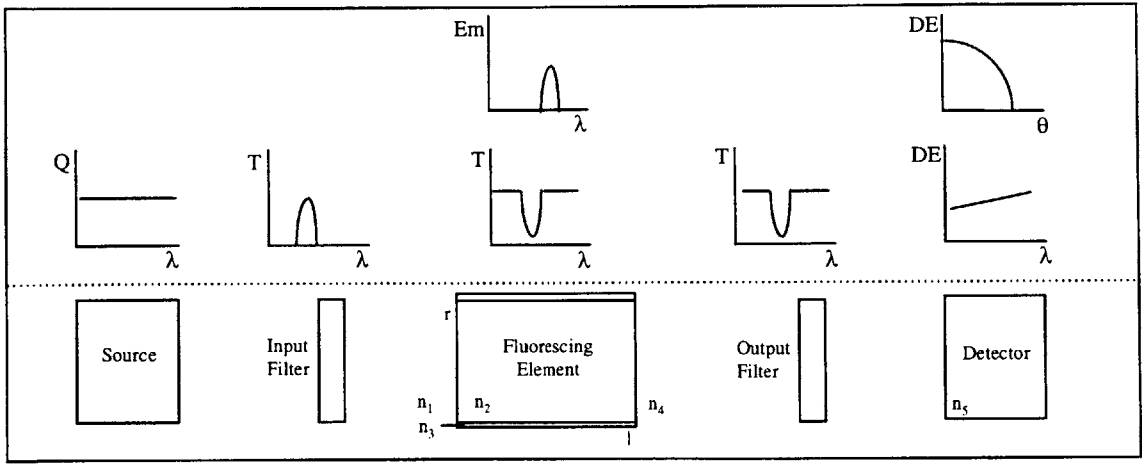
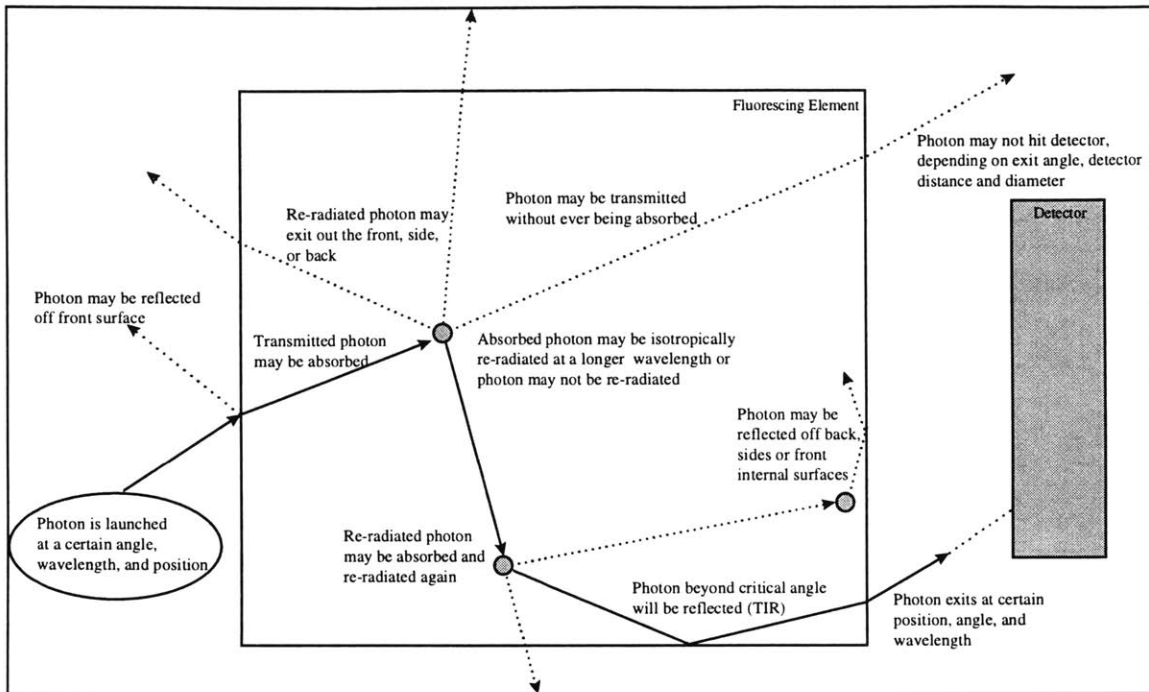


Figure 9- Specifications of Material Properties

## 3.20 Monte Carlo Process



**Figure 10- Monte Carlo Simulation Possibilities**

The Monte Carlo process allows each photon to travel through the material and experience a variety of interactions, as illustrated in Figure 10.

The user initiates the MC model by supplying the data described previously as well as the number of photons to be launched by the model. The MC model begins its operation by reading in all the relevant data files and parameters specified by the user. For each photon tracked through the model, an initial wavelength is chosen. The intensity versus wavelength data describing the source is multiplied, wavelength by wavelength, by the transmission versus wavelength data describing the input filter. The result is used as a probability function for wavelength selection. The photon then gets an initial direction

which is chosen from the data file describing the distribution of input angles. Finally, the photon is assigned a random initial position of entrance into the fluorescing element.

The indices of refraction of the fluorescing element and the surrounding medium determine, according to the Fresnel equations, the reflectivity of the front surface. The Fresnel equations<sup>30</sup> follow, with symbolic references as indicated in Figure 11:

$$R_{\text{perpendicular}} = (r_{\text{perpendicular}})^2$$

$$R_{\text{parallel}} = (r_{\text{parallel}})^2$$

where

$$r_{\text{perpendicular}} = (n_i \cos\theta_i - n_t \cos\theta_t) / (n_i \cos\theta_i + n_t \cos\theta_t)$$

$$r_{\text{parallel}} = (n_t \cos\theta_i - n_i \cos\theta_t) / (n_i \cos\theta_i + n_t \cos\theta_t)$$

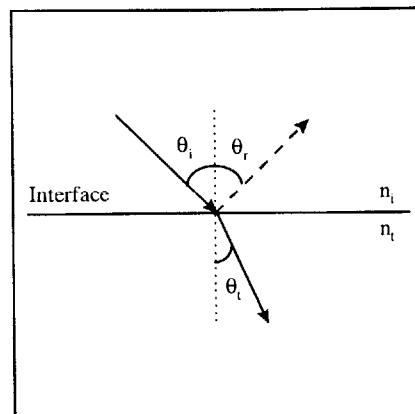


**Figure 11- Schematic of Boundary Interaction**

The reflectivity is also dependent on the polarization of incident light. Since photons in the MC model are assumed to be unpolarized, an average value of the reflectivity for perpendicular and parallel polarizations is used as a reflection probability:

$$R_{\text{average}} = \frac{1}{2} ( R_{\text{perpendicular}} + R_{\text{parallel}} )$$

As a result, a normally incident photon has about a four percent chance of being reflected off the front surface of a piece of glass ( $n = 1.5$ ) if it enters from air ( $n = 1.0$ ).

If a photon does not get reflected off the front surface and is transmitted into the fluorescing element, its direction is adjusted according to Snell's Law<sup>30</sup>:

$$n_i \sin\theta_i = n_t \sin\theta_t$$

Using this new direction and the starting location determined earlier, the path of the photon is determined. When the photon has gone the distance probabilistically determined by the absorption coefficient for that photon's wavelength, the end point of the photon's path is found. The end point is then compared with the boundaries of the cylindrical fluorescing element. If the end point lies outside of the cylinder, then the photon is considered to have hit the wall or end faces of the cylinder. (See Figure 12.)

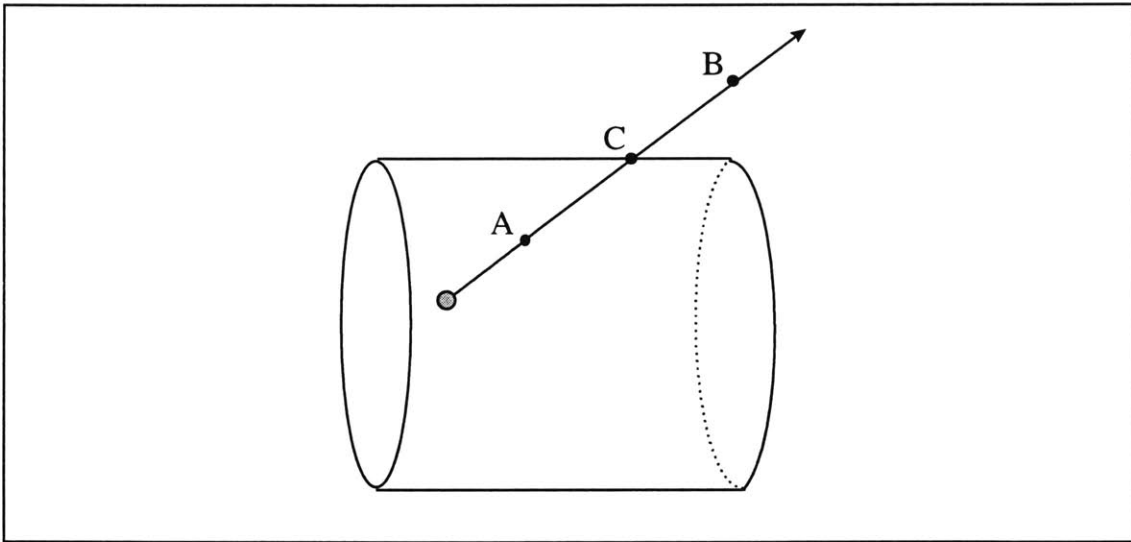


**Figure 12- Deciding if a Photon is Absorbed in the Material - The point of absorption is calculated and compared to the cylinder boundary. If the absorption point is at A, a real absorption occurred. If the absorption occurred at B, real absorption did not occur, and the point of interaction at the cylinder boundary, C, is determined.**

Again, indices of refraction dictate the photon's action at the boundary. The reflectivity of the boundary describes the probability of a photon getting reflected off the boundary. Assuming the index of refraction for the fluorescing element is greater than its

surroundings, such as in the case of glass in air, a critical angle exists for the boundary. If a photon hits the boundary at an angle greater than the critical angle (measured from the normal to the surface), then it will be reflected 100 percent of the time, a phenomenon commonly referred to as total internal reflection (TIR). In the MC model, photons which are transmitted through the side wall or back out the front surface are recorded as such. Photons which are transmitted through the back surface have their exit direction modified according to Snell's Law. The wavelength, position, and angle of the photon is noted so that the remainder of its path can be traced.

If a photon is absorbed in the fluorescing element before reaching a boundary, it has a certain chance of being re-radiated (determined by the fluorescence quantum efficiency). The chance, defined by the user, can vary widely with material. If the absorption event results in non-radiative decay, the absorbed photon is considered to have been lost to heat. Otherwise, a new photon is launched from the point of absorption. The re-radiation is assumed to be isotropic, having equal chance of radiating in any direction over  $4\pi$  steradians. The wavelength of the new photon is determined using the emission spectrum for the fluorescing material as a probability function. The photon's path is then traced as before.

Photons which exit out the back of the fluorescing element pass through the output filter and on to the detector. The transmission properties of the output filter define the probability that a photon of a particular wavelength will pass through the filter. Likewise, the detector efficiency defines the probability that the detector will register an incident photon.

The process is summarized by flowcharts in Appendix A.



### 3.30 Statistical Methods

The computer's built-in ability to generate random numbers is limited to uniformly choosing a real, random number between 0 and 1. Therefore, when non-uniform probability functions are required, it is necessary to transform the probability function into a cumulative density function (CDF). The CDF can be used to make a probabilistically weighted selection by applying the computer's 0 to 1, uniform random number generator<sup>27</sup>. Issues also arise when generating uniformly distributed circular and spherical coordinates using the computer's linear, one dimensional random number generator. The techniques used in applying the random number generator in the model are outlined in the following sections.

### 3.31 Initial Position

It may seem appropriate to use radius and angle coordinates to describe the initial position on the front surface of the cylinder since it is circular. However, if a radius is chosen uniformly between 0 and 1cm (assuming a cylinder with diameter 2cm) and an angle for that radius is chosen uniformly between 0 and  $2\pi$ , the result will not be a set of coordinates uniformly distributed over the circular face. Instead, there will be a density peak at the center of the face, trailing off at the edges of the circular face. One way to correct the distribution would be to determine non-linear probability distributions for choosing the radius and angle. Another way, is to use x and y coordinates, each chosen uniformly from  $-R$  to  $+R$  (where  $R$  refers to the radius of the cylinder), as shown in Figure 13. The result is a set of coordinates uniformly distributed over a square measuring  $2R$  on each side. By discarding any pair of coordinates which places the point outside of the circle of radius  $R$ , the remaining points make up a uniform distribution of points on the circle.

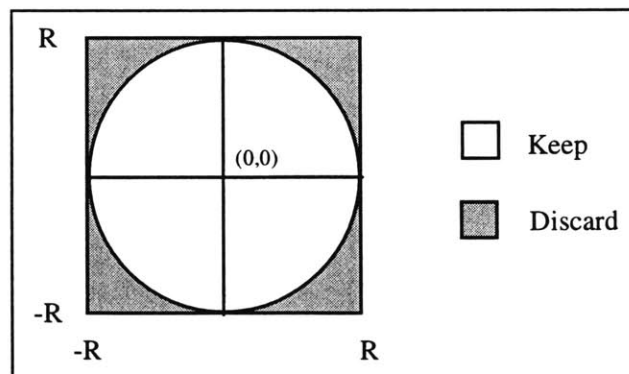


**Figure 13- Choosing a Random Start Location - Starting points chosen in the shaded area will be discarded and a new point will be chosen.**

### 3.32 Initial Wavelength

The combination of the source and initial filter determine the intensity for each wavelength of light impinging on the fluorescing element's front surface. A normalized set of this data comprises a probability distribution for the various possible initial wavelengths of photons entering the fluorescing element. A cumulative density function (CDF), shown in Figure 14, is built from this data. The  $n^{\text{th}}$  wavelength's CDF value is the sum of all the probabilities in the distribution for wavelengths up through the  $n^{\text{th}}$  wavelength divided by the sum of all the probabilities in the distribution. A random number is generated uniformly between 0 and 1 and matched to the closest CDF value. That CDF value will correspond to a particular initial wavelength.

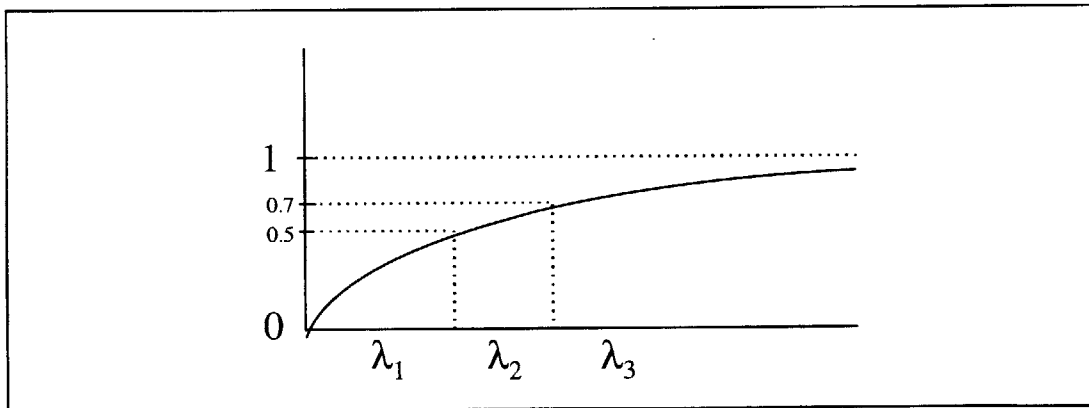


**Figure 14- Cumulative Density Function (CDF) - The CDF gives a weighted probability for a linear random number generator. A random number between 0.5 and 0.7 would correspond to a choice of  $\lambda_2$ .**

### 3.33 Initial Direction

The initial direction is chosen in a similar way as the initial wavelength in that a file describing the distribution of input angles is used to create a CDF. A random number between 0 and 1 is compared to the CDF to choose an initial direction in terms of an angle  $\theta$ , measured with respect to the optical axis of the cylinder. The angle  $\theta$  is then converted into a unit direction vector with components  $x$ ,  $y$ , and  $z$ . Since the cylindrical element is radially symmetric, an assumption is made that when converting the angle into a vector direction, the  $x$ -component of the vector can be set to zero, leaving just  $y$  and  $z$  components. (See Figure 15.)

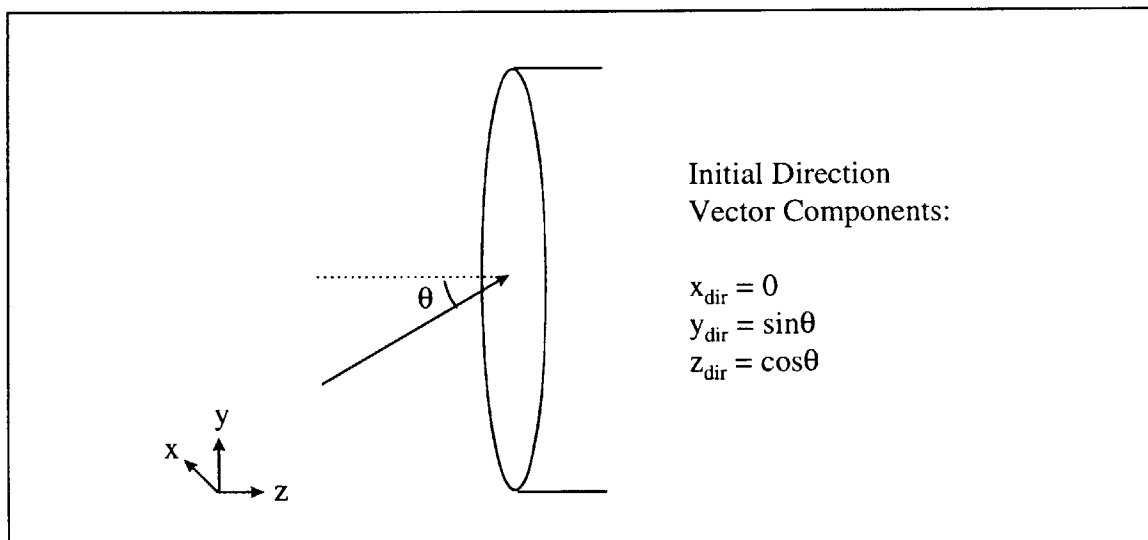


**Figure 15- Calculating Initial Direction - The initial direction is determined by choosing an initial angle,  $\theta$ , from a weighted probability function. The angle is then converted to vector components. The assumption is made that the results will be the same for a collimated bundle of rays at a certain angle as rays fixed in a certain cone angle, since the cylinder is radially symmetric.**

### 3.34 Distance to Absorption Point

The absorption coefficient for a particular wavelength is calculated from the material's transmission data for that wavelength. The absorption coefficient is used in the equation for absorption which describes the probability that a photon will be absorbed at a given distance. A random number is chosen and matched with the corresponding distance at which the absorption would take place, as shown in Figure 16.

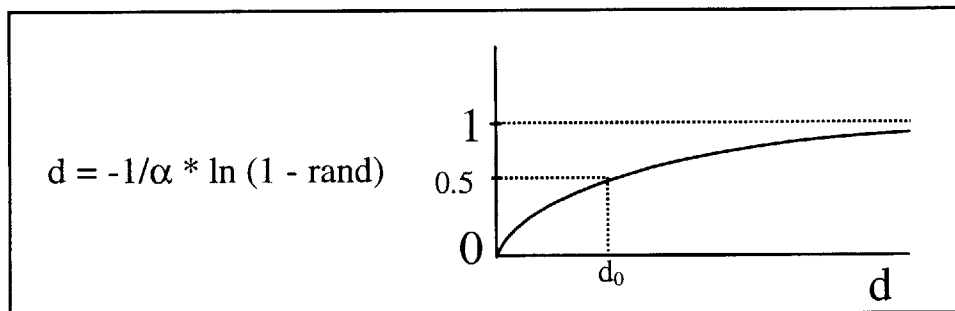


**Figure 16- Calculating the Distance a Photon Travels - The distance a photon travels is based on the absorption coefficient for the photon's wavelength,  $\alpha$ , and a random number chosen between 0 and 1, rand.**

### 3.35 Re-Radiation Direction

Choosing the direction of re-radiation is equivalent to choosing a point on a unit sphere. A technique similar to what is used for determining initial position is employed. Vector components x, y, and z are chosen independently using a uniform probability function in a range from -1 to 1. If the point described by the coordinates lies outside a sphere of radius 1, the point is discarded and a new point is chosen. Finally, the vector components are normalized so that the point lies on the unit sphere.

### 3.36 Re-Radiation Wavelength

The wavelength of a re-radiated photon is chosen in a similar way as the initial wavelength except that it is based on the fluorescing element's emission data. As before, the emission data is used as a probability density function (PDF) to indicate the probability that a photon will have a particular wavelength. The PDF is used to create a cumulative density function (CDF) which in turn matches a random number between 0 and 1 to a wavelength. An additional assumption for re-radiated photons is that the wavelength at which a photon re-radiates must be greater than the wavelength of the photon which was absorbed to create the opportunity for re-radiation. Thus, a different CDF exists for each possible wavelength of absorption.

## 3.40 Data Output

Since the Monte Carlo model tracks individual photons, it keeps a record of each photon's destination. Therefore, when 100,000 photons enter the model, all 100,000 must be accounted for, whether they exit the output surface, exit the side boundary, or just get absorbed and not re-radiated. Possible photon destinations are listed in Table 2

Reflected Off Front
Absorbed; Not Re-radiated
Exit Out Front; Direct
Exit Out Front; Fluorescent
Exit Out Side; Direct
Exit Out Side; Fluorescent
Exit Out Back; Direct
Exit Out Back; Fluorescent
Trapped Inside (>50 Reflections)

**Table 2- Possible Photon Destinations**

When a photon exits the output surface of the fluorescing element, it has properties of wavelength, angle, and position. The following sections describe the ways in which this data is collected for analysis.

## 3.41 Spectral Data

Photons exiting the output surface are either direct photons or fluorescent photons and are counted in a similar way, but in two separate categories. A histogram representing the number of photons exiting at a particular wavelength is built up as the wavelength of each exiting photon is recorded. When the histogram is complete, it is possible to say that, for example, 50 photons exited at 500nm, but it is not possible to say at what wavelength the 5,000<sup>th</sup> photon exited.

## 3.42 Angular Data

The angular characteristics of photons exiting the output surface are recorded in almost the same way as the photon's spectral characteristics. A histogram of the number of photons exiting at a particular cone is built as each photon exits. The cone angle of a particular photon is calculated by taking the inverse cosine of the dot product of the direction vector of the exiting photon and the normal vector, which is the normal to the output surface. The exit angle of a photon is independent of the photon's exit position.

A further modification to the data can be made for ease of comparison to a Lambertian radiator. (A Lambertian radiator varies as  $\cos\theta$ , where  $\theta$  is the angle from the normal<sup>12</sup>.) The photons exiting at a particular angle can be divided by the differential surface area subtended by that solid angle and the solid angle of one more degree,  $2\pi(\cos\theta_1 - \cos\theta_2)$ . The result is photons per steradian.

## 3.43 Positional Data

Saving the exit coordinates for each photon would create an overwhelming amount of data which may not even be instructive. The output surface is therefore divided into annuli of equal width. As each photon exits, the annulus through which the photon exited is recorded. Before this data is presented, the total number of photons in a particular annulus is divided by the area of that annulus to calculate photons per area in an annulus of a particular radius.



### 3.44 Trapped Photons

One of the possible destinations for a photon in the model is to be trapped. A photon is considered trapped when it has experienced more than 50 reflections. The maximum number of reflections is an arbitrary choice, partially dependent on the computer's ability to track a reflecting photon forever (stack space), and partially because it is expected that in a real life situation, the photon would have been scattered long before it was reflected 50 times. Scattering might take place in either the bulk of the material or at boundaries. Since boundaries in the model are perfect surfaces and bulk scattering events are not considered, high numbers of reflections before escape are possible in the model.

There are two probable ways a photon may become trapped, as illustrated in Figure 17. One way is a longitudinal pattern of reflection by which the photon reflects off the side boundary, exit surface, side boundary, and entrance surface, and then repeats. Indices of refraction of the material and boundaries will determine angles at which a photon reflects, and it is certainly possible to have a combination for which a range of certain angled photons will become trapped.

The second way a photon may be trapped is in a transverse plane, as a photon bends around the curved side boundary. This could happen in three dimensions, but for illustrative purposes, consider the action in a circle, as in Figure 18. A photon emitted in the center of the circle will hit the circle boundary normal to the tangent at that point on the circle, and will be transmitted. As the position of the photon emission moves toward the circle boundary, a range of angles develops, over which a photon will reflect (via TIR)

off the circle boundary. Reflected photons will continue to reflect every time they hit the circle boundary, and are good candidates for becoming trapped photons.

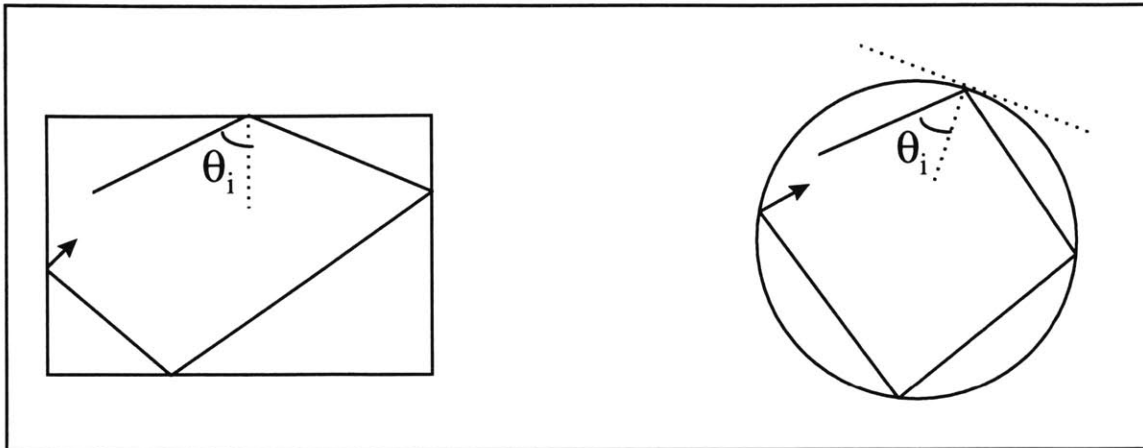


**Figure 17- Trapping Geometries - A Photon may become trapped in a longitudinal or transverse plane if  $\theta_i$  is greater than the critical angle for that boundary**

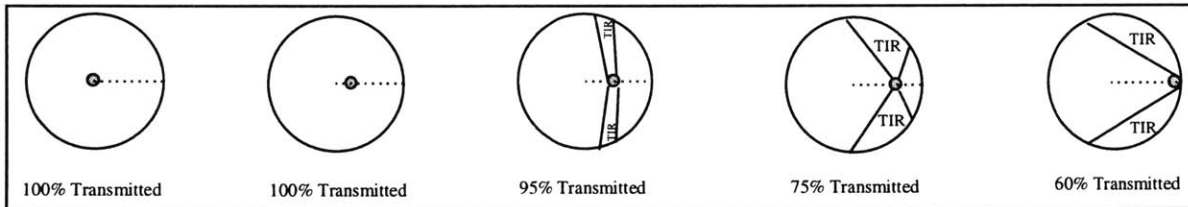


**Figure 18- Total Internal Reflection (TIR) Preventing Transmission - As the point of emission moves towards the edge of the circle boundary, the range of emission angles which will result in TIR increases and the number of photons which will be transmitted through the boundary decreases.**

## 4.0 Model Parameter Effects

The model, as described earlier, is capable of supporting a large number of model parameter combinations. Specific choices for parameters would depend on the optical system of which the fluorescent element was a part. The following sections illustrate some of the major factors which would contribute to observed output from the model. Specific cases are discussed, demonstrating the model's utility. The cases are divided into categories to emphasize the major factors contributing to a material's fluorescence behavior, as shown in Table 3.

Spectral Characteristics	Boundary Effects	Input Angle	Diameter of Input	Length/Diameter Ratio	Detector Configuration
Separated	Air	$\theta_i < \theta_A$	Flooded $d_1/d_2 = 1$	$l/d > 1$	Coupled
Overlapping	Cladding	$\theta_i > \theta_A$	Beam $d_1/d_2 < 1$	$l/d = 1$	Uncoupled
	Diffuse Reflective		Spot $d_1/d_2 \ll 1$	$l/d < 1$	

**Table 3- Configurations Considered**

To demonstrate the effect of a material's spectral characteristics, two possible cases are shown, one with the excitation and emission spectra separated and one with the spectra overlapping. Boundary Effects are shown for three possible boundary conditions. The effects of input angle are shown through combined results from several cases, each for a particular input angle. Three cases illustrate the effect of varying the input beam diameter. The length/diameter ratio is shown to have an effect with cases of various ratios. Finally, an optically coupled case shows an effect of detector distance and index matching.

No attempt was made to provide results for all of the possible permutations of parameters. These cases merely provide insight into effects an optical designer might consider when engineering an optical system.

While the model will accept curves of any shape for inputs, certain shapes have been chosen for the cases run. These shapes include a monochromatic source, all-band transmissive input and output filters, a detector efficiency of 100% at all wavelengths and angles, and gaussian excitation and emission curves. The Gaussian curve, illustrated in Figure 19, is defined by the wavelength of its peak and its full width half maximum (FWHM) value. Fluorescence quantum efficiency, the probability that an absorbed photon will result in a re-emission event, is another parameter of this model. For the following illustrative cases, a value of 80% was chosen. If varied, the quantum efficiency would affect the magnitude of the fluorescence output, but would do so equally for all cases.

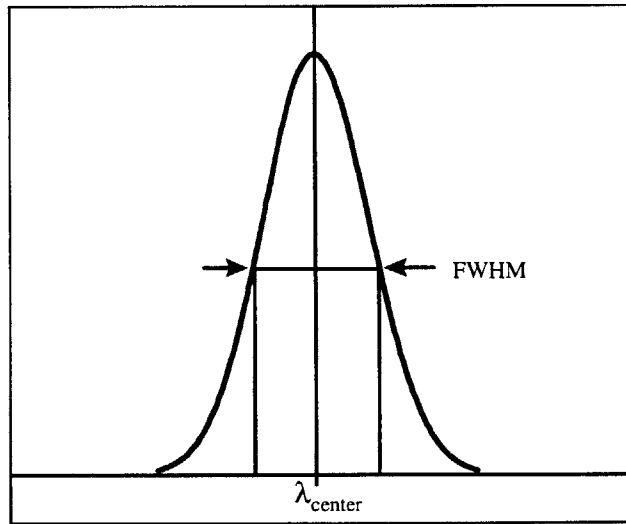


**Figure 19- Gaussian Distribution**

## 4.1 Spectral Characteristics

Spectral Characteristics	Boundary Effects	Input Angle	Diameter of Input	Length/Diameter Ratio	Detector Configuration
Separated Overlapping	Air	$\theta_i < \theta_A$	Flooded $d_1/d_2 = 1$	$l/d > 1$	Coupled
	Cladding	$\theta_i > \theta_A$	Beam $d_1/d_2 < 1$	$l/d = 1$	Uncoupled
	Diffuse Reflective		Spot $d_1/d_2 \ll 1$	$l/d < 1$	

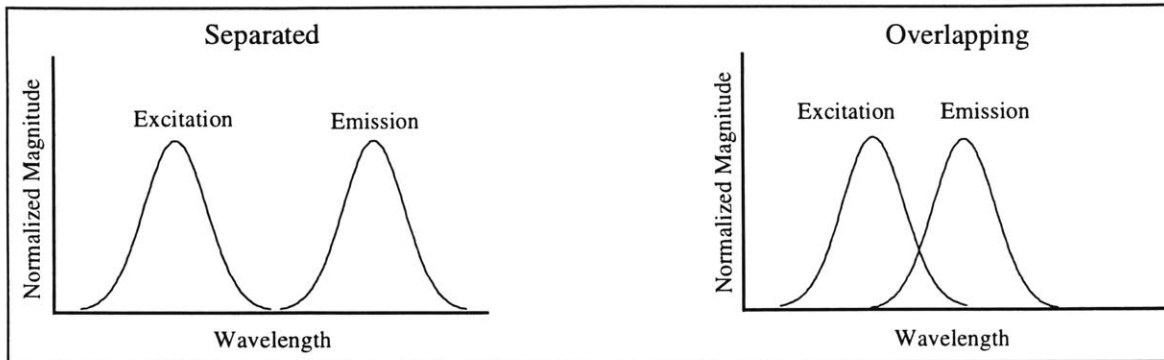


**Figure 20- Excitation and Emission Spectra Configurations - A material's excitation and emission spectra may be separated or overlapped.**

The material chosen for the fluorescing element has certain spectral characteristics which are independent of the source radiation impinging upon the material. The spectral characteristics are described by two spectra, namely, the excitation spectrum and the emission spectrum. The excitation spectrum describes the wavelengths at which the material may be excited by input radiation, and the emission spectrum describes the wavelengths at which photons that have been absorbed will be re-emitted. As mentioned earlier, in the discussion of the model, an assumption is made that the excitation can be derived from the absorption properties of the material as long as there is only a single fluorophore.

Two distinct cases of a material's spectral characteristics will be considered. The excitation and emission spectra for a material may either be separated in wavelength, or

overlapping in wavelength, as illustrated in Figure 20. The input parameters for the two cases considered are summarized in Table 4.

Parameters	Spectral Characteristics Test Cases	
	Separated	Overlapping
Number of Photons	1M	1M
Quantum Efficiency	80%	80%
Excitation/Input	248nm	248nm
Material Index	n=1.5	n=1.5
Excitation/Emission Spectra	Separated	Overlapping
Entrance Surface Boundary	Air	Air
Side Boundary	n=1.3	n=1.3
Exit Surface Boundary	Air	Air
Input Angle	0 degrees	0 degrees
Input Beam Diameter	Flooded	Flooded
Length	Varied	Varied
$\alpha$	Varied	Varied
Material Diameter	1.0 cm	1.0 cm
Detector Distance	0 cm	0 cm
Detector Diameter	1.0 cm	1.0 cm
Detector Index	n=1.0	n=1.0

**Table 4- Spectral Characteristics Test Cases**

In the separated case, a photon may be absorbed and re-emitted only once, since the wavelength of the re-emitted photon is no longer within the material's excitation region, as seen in Figure 21. One can see that with separated excitation and emission spectra, direct photons exit the material at the same wavelength they were input and fluorescent photons fit to the shape of the emission spectrum. The relative magnitude of fluorescent photons for various lengths is also apparent. The 1.0 cm case and 5.0 cm case do not vary much in magnitude. The lack of variation is due to the high absorption coefficient which, at a certain length, will lead to the absorption of almost all of the input photons. Thus, even if the material is made longer, there are few additional photons to be absorbed and fluoresced.

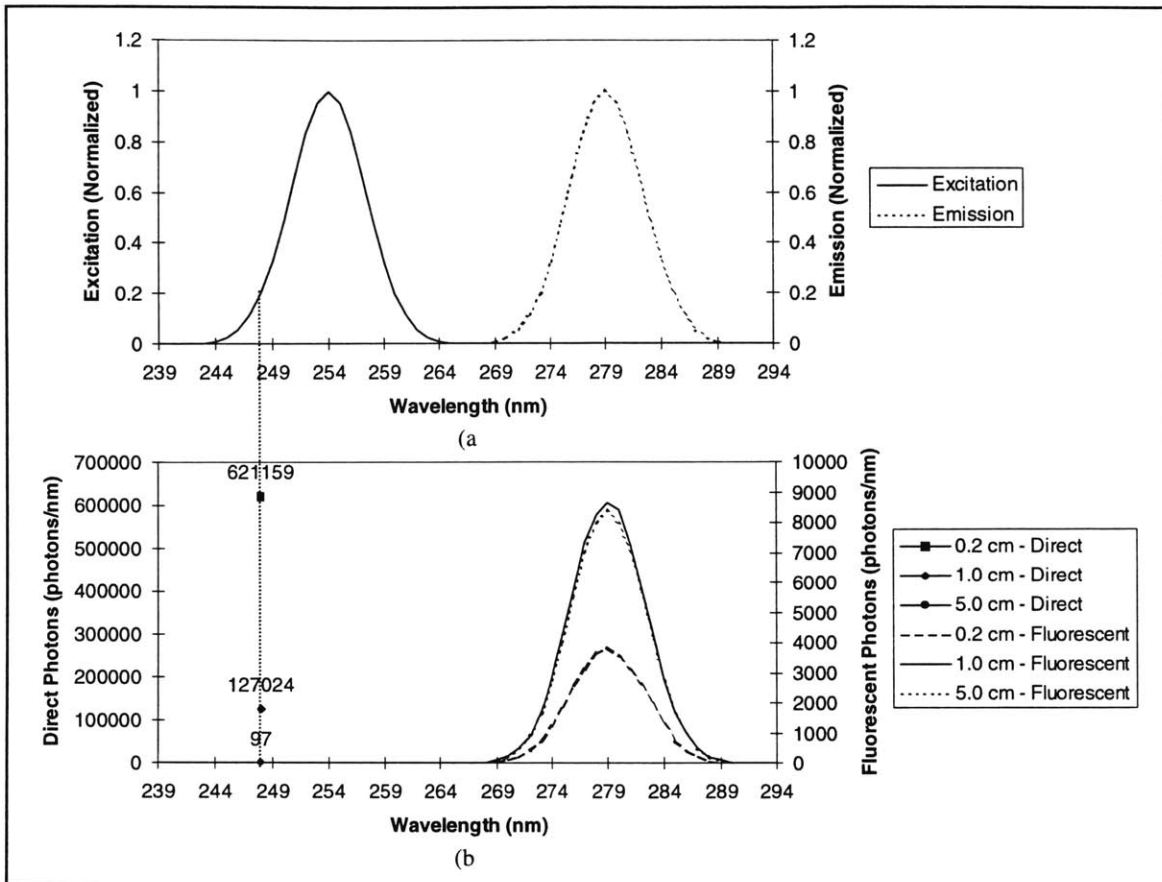


**Figure 21-Emission for Separated Spectra - (a) Fluorescent Material Properties, Separated Spectra (b) Direct and Fluorescent Photons Exiting Output Surface vs. Wavelength for Various Lengths (1,000,000 Photons; Diameter = 1.0cm; Peak Absorption Coefficient =  $10\text{cm}^{-1}$ ; Initial Excitation 248nm; Cladded Boundary;  $n_i/n_c = 1.5/1.3$ )**

In the overlapping case, a photon may be absorbed and re-emitted several times if the wavelength of the re-emitted photon remains inside the material's excitation region. The characteristics of the source radiation will become a factor in determining the shape of the emission. If a monochromatic source excites the material in the region where the material's excitation and emission spectra overlap, then the characteristic emission will only be observed for wavelengths greater than the source. A broadband source spanning wavelengths in the overlapping region would distort the characteristic spectrum, since a broadband source may be considered a superposition of monochromatic sources.

Multiple absorptions in the overlapping case are very similar to having a broadband source, since re-emitted photons have new, longer wavelengths. The difference is that the re-emitted photons originate inside the material. The same distortion of the emission curve expected for a broadband source is therefore expected for a monochromatic source when multiple absorptions occur. The distortion process in this case is known as self-absorption in the material. As the optical path (the product of the absorption coefficient and length of the cylinder) in a material increases, the portion of the fluorescence emission spectra which overlaps the excitation will be increasingly eroded, while the non-overlapping portion will continue to fit the characteristic emission spectrum, as seen in Figure 22. The erosion of the left side of the fluorescent emission is most apparent when the emission for various path lengths ( $\alpha l$ ) is normalized, as in Figure 22(c).



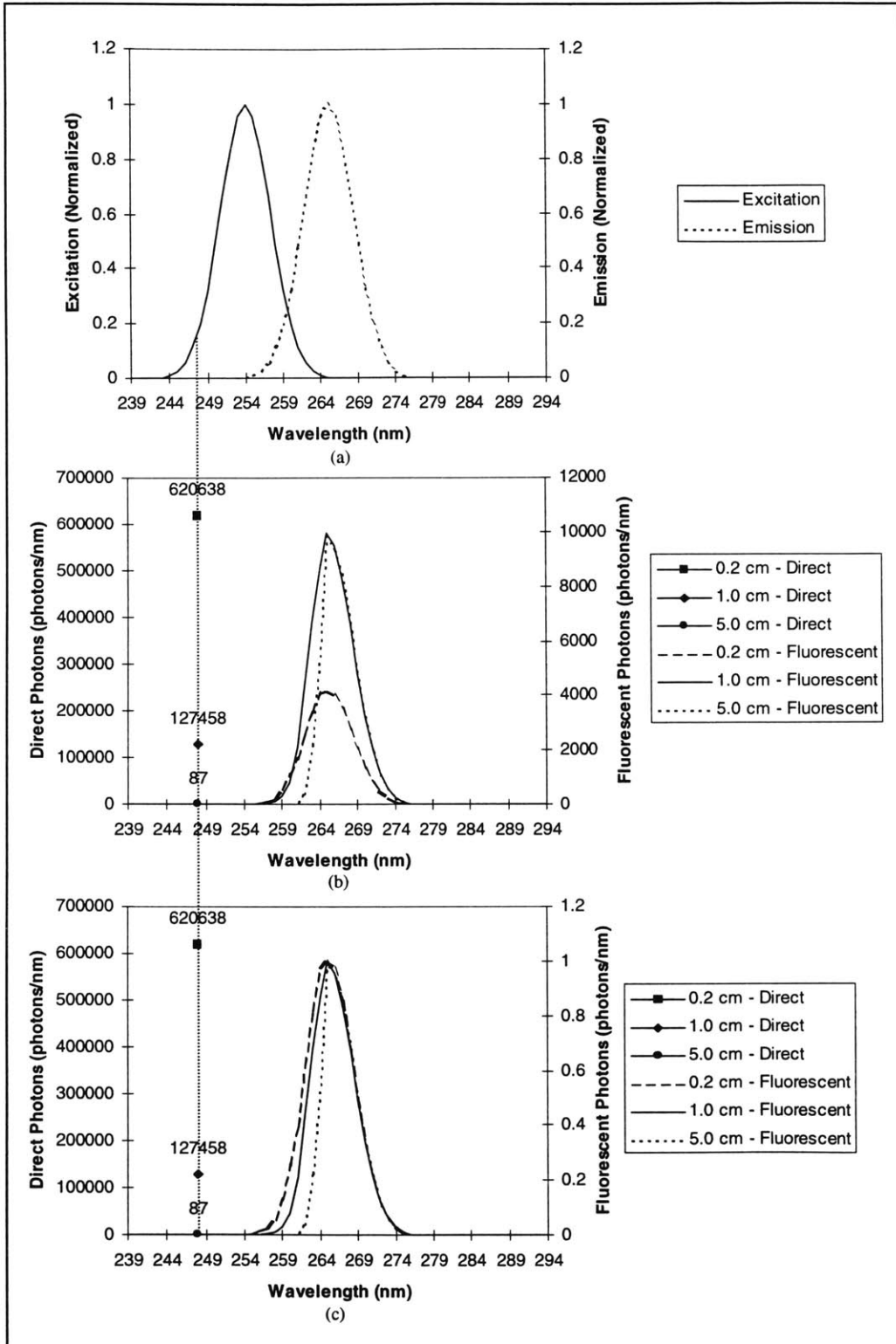


**Figure 22- Emission for Overlapping Spectra - (a) Fluorescent Material Properties, Overlapping Spectra (b) Direct and Fluorescent Photons Exiting Output Surface (c) Normalized Fluorescent Output (1,000,000 Photons; Diameter = 1.0cm; Peak Absorption Coefficient =  $10\text{cm}^{-1}$ ; Initial Excitation 248nm; Cladded Boundary;  $n_i/n_c = 1.5/1.3$ )**

The effect of self absorption on the magnitude of fluorescence exiting the output surface is also apparent in Table 5 and Table 6. At shorter lengths, the difference in output fluorescence magnitude is small, but at 5.0 cm, the difference becomes more significant.

Separated Spectra					
Length	0.2 cm	0.5 cm	1.0 cm	2.0 cm	5.0 cm
Reflected Off Front	40342	39799	39934	39878	39979
Absorbed; Not Re-radiated	64509	122048	165607	188916	192538
Exited Out Front; Direct	16561	4980	757	20	0
Exited Out Front; Fluorescent	31762	58156	76026	84060	85553
Exited Out Side; Direct	0	0	0	0	0
Exited Out Side; Fluorescent	176593	342766	473408	546317	560383
Exited Out Back; Direct	621159	342074	127024	17775	97
Exited Out Back; Fluorescent	31730	57635	72507	72902	69869
Trapped Inside (>50 Reflections)	17344	32542	44737	50132	51581

**Table 5- Monte Carlo Test Results for Separated Spectra**

Overlapping Spectra					
Length	0.2 cm	0.5 cm	1.0 cm	2.0 cm	5.0 cm
Reflected Off Front	40052	39639	39894	40083	39881
Absorbed; Not Re-radiated	71094	136458	186842	214039	219039
Exited Out Front; Direct	16756	5031	711	16	0
Exited Out Front; Fluorescent	33301	59801	76827	84553	85631
Exited Out Side; Direct	0	0	0	0	0
Exited Out Side; Fluorescent	173027	336216	468296	545053	565310
Exited Out Back; Direct	620638	342294	127458	17516	87
Exited Out Back; Fluorescent	33183	58098	69428	64150	54213
Trapped Inside (>50 Reflections)	11949	22463	30544	34590	35839

**Table 6- Monte Carlo Test Results for Overlapping Spectra**

A person seeking to maximize fluorescence would choose a material whose spectra were separated to avoid the effects of self absorption. If such a material were unavailable, then a shorter length would be chosen for the material with overlapping spectra. A person seeking to minimize fluorescence may be able to take advantage of the self-absorption effect by choosing a material with overlapping spectra. These conclusions are summarized in Table 7.

Parameter	Maximize Fluorescence	Minimize Fluorescence
Separated Spectra		<b>X</b>
Overlapping Spectra	<b>X</b>	

**Table 7- Parameter Choices for Each Goal**

## 4.2 Boundary Effects

Spectral Characteristics	Boundary Effects	Input Angle	Diameter of Input	Length/Diameter Ratio	Detector Configuration
Separated	Air	$\theta_i < \theta_A$	Flooded $d_1/d_2 = 1$	$l/d > 1$	Coupled
Overlapping	Cladding	$\theta_i > \theta_A$	Beam $d_1/d_2 < 1$	$l/d = 1$	Uncoupled
	Diffuse Reflective		Spot $d_1/d_2 \ll 1$	$l/d < 1$	

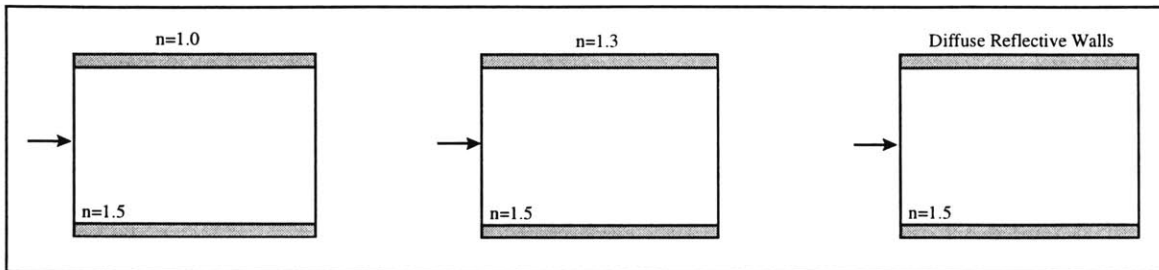


**Figure 23- Side Boundary Configurations - The side boundary may be air, a cladding, or diffuse reflective.**

There are several ways in which the side boundaries of a fluorescing material may be configured to affect the magnitude and angular characteristics of photons exiting the output surface. The following side boundary configurations, as shown in Figure 23, will be considered: a side boundary with no treatment at all (an air boundary), a side boundary surrounded by a cladding, much like an optical fiber, and a side boundary coated so that it would act as a diffuse reflective surface. The input parameters for the three cases considered are summarized in Table 8.

Parameters	Boundary Effects Test Cases		
	Cladded	Air	Diffuse Reflective
Number of Photons	1M	1M	1M
Quantum Efficiency	80%	80%	80%
Excitation/Input	254nm	254nm	254nm
Material Index	n=1.5	n=1.5	n=1.5
Excitation/Emission Spectra	Separated	Separated	Separated
Entrance Surface Boundary	Air	Air	Air
Side Boundary	Cladded n=1.3	Air n=1.0	Diffuse Reflective
Exit Surface Boundary	Air	Air	Air
Input Angle	0 degrees	0 degrees	0 degrees
Input Beam Diameter	Flooded	Flooded	Flooded
Length	Varied	Varied	Varied
$\alpha l$	Varied	Varied	Varied
Material Diameter	1.0 cm	1.0 cm	1.0 cm
Detector Distance	0 cm	0 cm	0 cm
Detector Diameter	1.0 cm	1.0 cm	1.0 cm
Detector Index	n=1.0	n=1.0	n=1.0

**Table 8- Boundary Effects Test Cases**

With an air or cladded side boundary, the reflectance of that surface is determined by the Fresnel equations as discussed in Section 3.2 . An air side boundary, for example, allows a greater range of angles for which a photon will totally internally reflect (TIR) than a cladded boundary would allow. The result is a decrease in the number of photons which exit through the side, as indicated by the results in Table 9 and Table 10.

Cladded Side Boundary					
Length	0.2 cm	0.5 cm	1.0 cm	2.0 cm	5.0 cm
Reflected Off Front	40012	40397	39830	40234	40294
Absorbed; Not Re-radiated	166903	190689	191914	192206	192450
Exited Out Front; Direct	723	2	0	0	0
Exited Out Front; Fluorescent	82416	91577	91858	91473	90883
Exited Out Side; Direct	0	0	0	0	0
Exited Out Side; Fluorescent	458590	532528	545984	552705	554055
Exited Out Back; Direct	124982	6142	75	46	48
Exited Out Back; Fluorescent	81677	87688	79487	72197	70568
Trapped Inside (>50 Reflections)	44697	50977	50852	51139	51702

**Table 9- Monte Carlo Test Results for Cladded Side Boundary**

Air Side Boundary					
Length	0.2 cm	0.5 cm	1.0 cm	2.0 cm	5.0 cm
Reflected Off Front	39756	39878	39946	39878	40203
Absorbed; Not Re-radiated	166312	190855	192037	192569	191554
Exited Out Front; Direct	691	0	0	0	0
Exited Out Front; Fluorescent	85097	97016	97598	97547	97831
Exited Out Side; Direct	0	0	0	0	0
Exited Out Side; Fluorescent	297126	339172	340963	341198	342036
Exited Out Back; Direct	124808	6340	92	54	55
Exited Out Back; Fluorescent	84853	97042	98091	97269	97570
Trapped Inside (>50 Reflections)	201357	229697	231273	231485	230751

**Table 10- Monte Carlo Test Results for Air Side Boundary**

A diffuse reflective side boundary does not allow any photons to exit the side by definition. (For the model, it is assumed that when a photon hits a diffuse reflective surface, it is reflected at a random angle independent of the incident angle.) Thus photons are forced to exit the entrance or output surfaces, dramatically increasing the number of photons exiting the output surface compared to the air or cladded cases, as seen Table 11. Since most of the absorptions occur closer to the entrance surface, the number of photons exiting the entrance surface is greater than the number exiting the output surface.

Diffuse Reflective Side Walls					
Length	0.2 cm	0.5 cm	1.0 cm	2.0 cm	5.0 cm
Reflected Off Front	39924	39940	40069	40100	40105
Absorbed; Not Re-radiated	167021	190419	192349	192259	191981
Exited Out Front; Direct	628	3	0	0	0
Exited Out Front; Fluorescent	333200	391114	414624	475554	566825
Exited Out Side; Direct	0	0	0	0	0
Exited Out Side; Fluorescent	0	0	0	0	0
Exited Out Back; Direct	124437	6275	70	49	62
Exited Out Back; Fluorescent	332424	372004	352699	290978	177161
Trapped Inside (>50 Reflections)	2366	245	189	1060	23866

**Table 11- Monte Carlo Test Results for Diffuse Reflective Boundary**

The angular distribution of fluorescent photons exiting the output surface is different for each of the three boundary conditions, as shown in Figure 24. With an air side boundary, the angular distribution is similar to a Lambertian distribution. With a clad side boundary, more photons exit the side boundary, reducing the number of high-angled photons and distorting the angular distribution away from the Lambertian. The higher the index of the cladding, the more pronounced the effect will be. The effect of diffuse reflective side walls is significant. As the  $l/d$  ratio increases (in Figure 24  $l/d=5$ ), the angular width of the fluorescent photon distribution narrows.

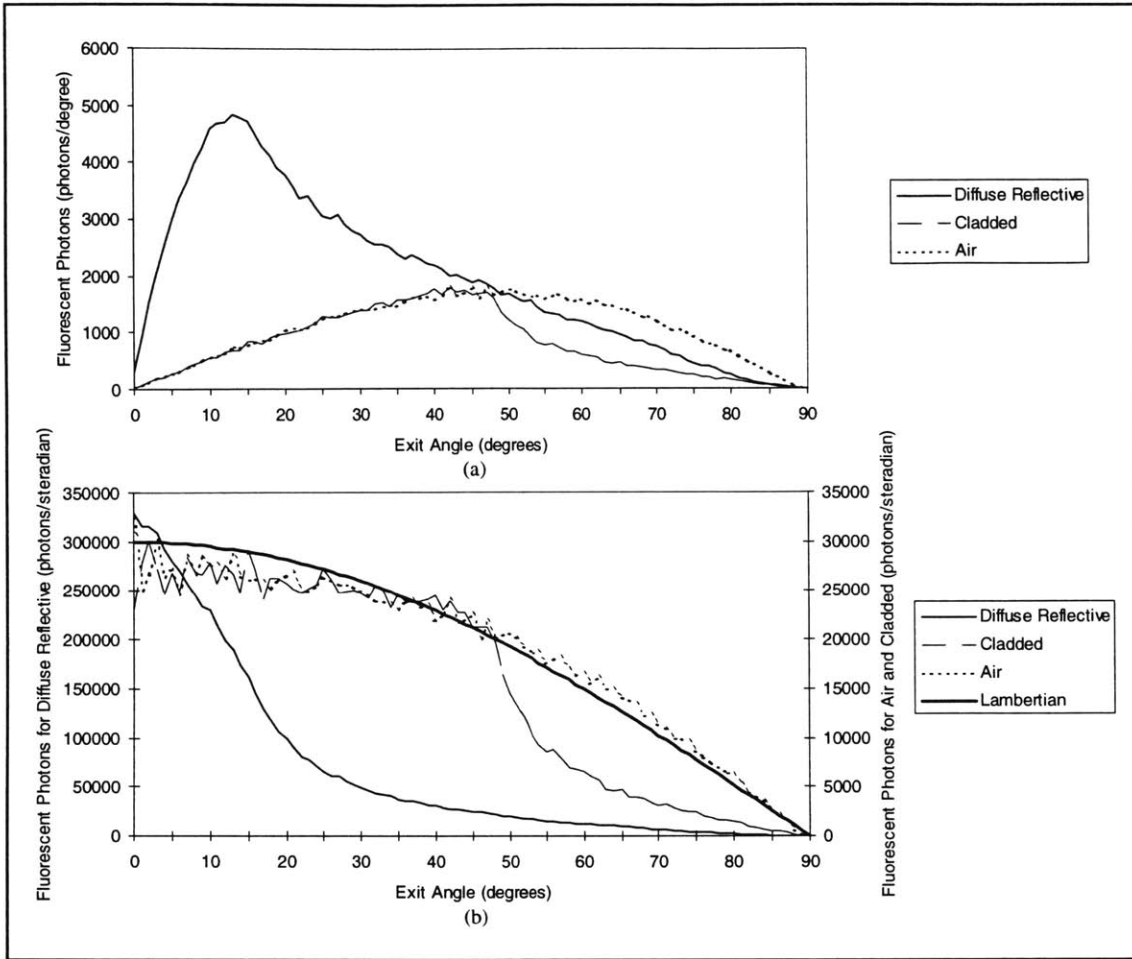


**Figure 24- Angular Distribution of Fluorescent Photons (a) Photons per Degree (b) Photons per Steradian (1,000,000 Photons; Separated Excitation/Emission Spectra; Diameter = 1.0cm; Length = 5.0cm; Peak Absorption Coefficient =  $10\text{cm}^{-1}$ ; Initial Excitation 254nm;  $n_i/n_c = 1.5/1.3$ , for Cladded Case)**



A person wishing to maximize the number of fluorescent photons exiting the output surface would choose diffuse reflective side walls and would treat the entrance surface with a coating which would reflect fluorescent photons back into the material. With this setup, all of the fluorescent photons would exit the output surface. A person seeking to minimize fluorescence would choose to put a cladding on the side boundary. A summary of these choices is presented in Table 12.

Parameter	Maximize Fluorescence	Minimize Fluorescence
Air Boundary		
Cladded Boundary		<b>X</b>
Diffuse Reflective Boundary	<b>X</b>	

**Table 12- - Parameter Choices for Each Goal**

## 4.3 Input Angle

Spectral Characteristics	Boundary Effects	Input Angle	Diameter of Input	Length/Diameter Ratio	Detector Configuration
Separated	Air	$\theta_i < \theta_A$	Flooded $d_1/d_2 = 1$	$l/d > 1$	Coupled
Overlapping	Cladding	$\theta_i > \theta_A$	Beam $d_1/d_2 < 1$	$l/d = 1$	Uncoupled
	Diffuse Reflective		Spot $d_1/d_2 \ll 1$	$l/d < 1$	

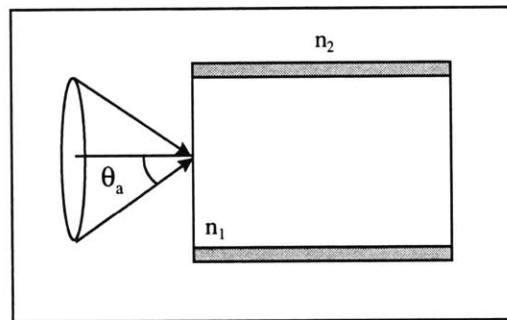


**Figure 25- Input Angle Configuration - The input angle may be either inside or outside the acceptance cone.**

The model will accept any input angle or angular distribution, as illustrated in Figure 25. This section will focus specifically on a collimated beam input at certain angles.

The effect of source radiation input angle are predicted by classical optics equations, particularly those for Numerical Aperture and acceptance angle. The Numerical Aperture is solely dependent on the indices of refraction of the material and its cladding, assuming the material is in air<sup>12</sup>:

$$NA = (n_1^2 - n_2^2)^{1/2}$$

The acceptance angle is simply:

$$\theta_a = \sin^{-1}(NA)$$

Radiation input at angles within the acceptance cone will be totally internally reflected at the side wall. In the model, photons exiting the output surface without ever having been absorbed will exit at the same angle that they were input (e.g. a photon input at 10 degrees will exit at 10 degrees). The photon may spiral around inside the material, but its angle with respect to the optical axis will remain constant.

Because the effect of input angle is dependent on the boundary condition, three cases, each with a different boundary condition, are considered. They are summarized in Table 13.

Parameters	Input Angle Test Cases		
	Cladded	Air	Diffuse Reflective
Number of Photons	1M	1M	1M
Quantum Efficiency	80%	80%	80%
Excitation/Input	254nm	254nm	254nm
Material Index	n=1.5	n=1.5	n=1.5
Excitation/Emission Spectra	Separated	Separated	Separated
Entrance Surface Boundary	Air	Air	Air
Side Boundary	Cladded n=1.3	Air n=1.0	Diffuse Reflective
Exit Surface Boundary	Air	Air	Air
Input Angle	Varied	Varied	Varied
Input Beam Diameter	Flooded	Flooded	Flooded
Length	1.0 cm	1.0 cm	1.0 cm
$\alpha l$	2	2	2
Material Diameter	1.0 cm	1.0 cm	1.0 cm
Detector Distance	0 cm	0 cm	0 cm
Detector Diameter	1.0 cm	1.0 cm	1.0 cm
Detector Index	n=1.0	n=1.0	n=1.0

**Table 13- Input Angle Test Cases**

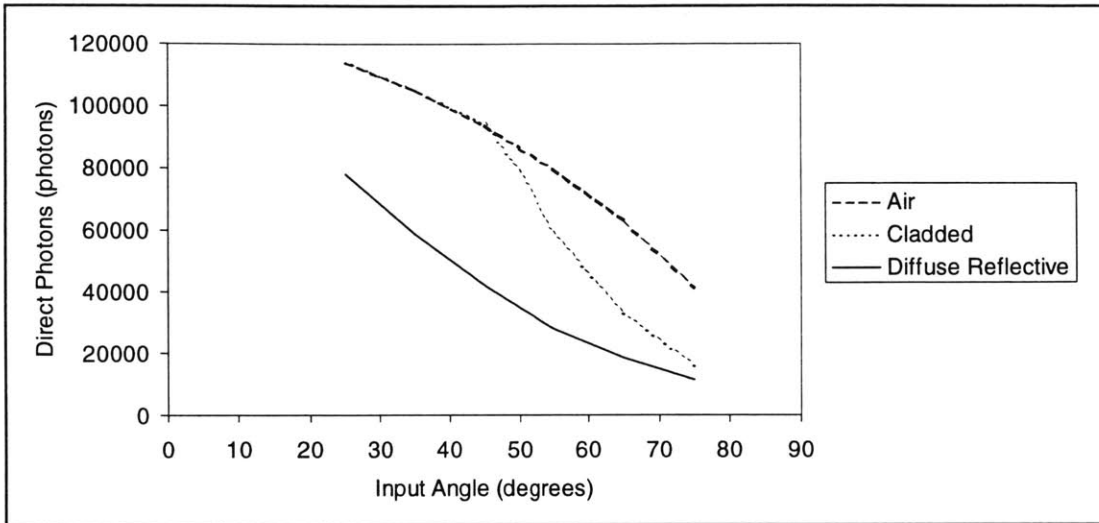


**Figure 26- Direct Photons Exiting Output Surface vs. Input Angle for Various Side Boundary Conditions (1,000,000 Photons; Separated Emission/Excitation; Diameter = 1.0cm; Length = 1.0cm; Peak Absorption Coefficient =  $2\text{cm}^{-1}$ ; Initial Excitation=254nm;  $n_i/n_c = 1.5/1.3$ , for Cladded Case)**

When the material has no cladding, air makes up the side boundary, and the acceptance angle is 90 degrees, meaning that every non-absorbed photon which hits the side wall will be reflected. As the angle of input increases from 0 to 90 degrees with respect to the normal to the entrance surface, the number of photons directly transmitted through the output surface of the material will decrease, assuming a fixed  $\alpha l$ , as seen in Figure 26. The transmission reduction is due to the longer path length which higher angled photons must travel before exiting the output surface and is equivalent to increasing the length,  $l$ , in  $e^{-\alpha l}$ , by a factor of  $1/\cos\theta_i$ , where  $\theta_i$  is the angle of the photon just after entering the material.

The same transmission loss will be observed for a cladded material for angles up to the acceptance angle for that particular combination of material and cladding. Beyond the acceptance angle, transmission through the output surface is even further reduced by the

loss of photons out of the side wall. The acceptance angle breakpoint is apparent in Figure 26. The acceptance angle for a material of index 1.5 and cladding of index 1.3 is about 49 degrees.

The concept of acceptance angle does not apply to a material with diffuse reflective side boundaries since all photons which impact the side will be reflected. Transmission loss will be similar to the air boundary case, as seen Figure 26, which also is not limited by an acceptance angle.

Whether the side boundary is cladded, uncladded or diffuse reflective, the angular distribution of fluorescent photons exiting the output surface will remain the same, as shown in Figure 27 and Figure 28. This is due to the fact that once a photon is absorbed, its incident angle is irrelevant as the new photon will be re-radiated isotropically. Photons input at a certain angle will either exit the material at the same angle or be absorbed. The diffuse boundary case has a small exception, however. In this case, the angular distribution of directly transmitted photons will be peaked at the input angle of the photon, but will also have a Lambertian-like distribution at other wavelengths, as seen in Figure 28(b). The distribution is due to photons which hit the wall and are reflected in a random direction.

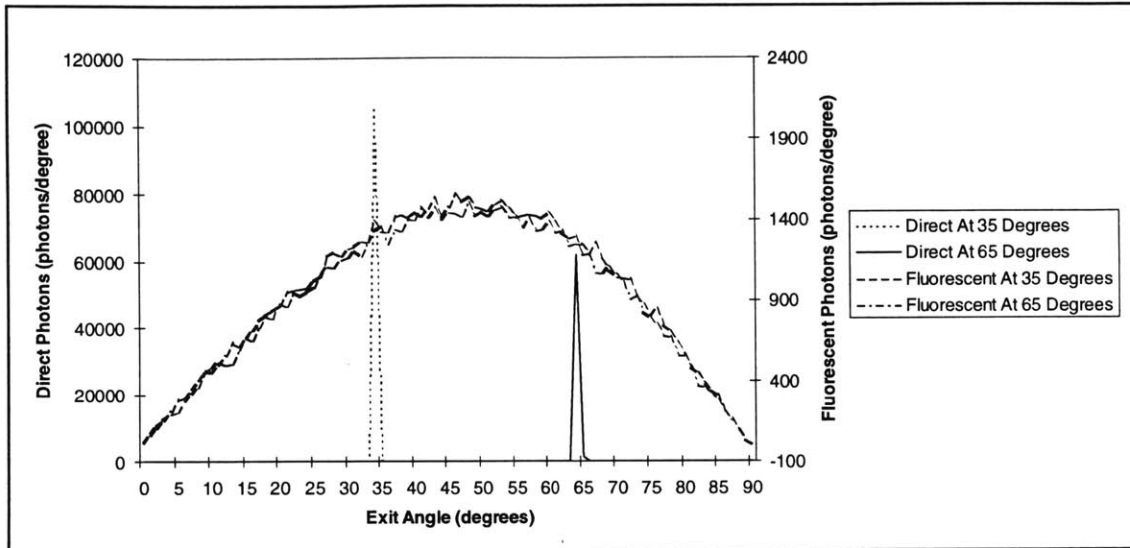


**Figure 27- Angular Distribution of Direct and Fluorescent Photons for Two Input Angles (Air Side Boundary; 1,000,000 Photons; Separated Emission/Excitation; Diameter = 1.0cm; Length = 1.0cm; Peak Absorption Coefficient =  $2\text{cm}^{-1}$ ; Initial Excitation=254nm;  $n_i/n_c = 1.5/1.0$ )**

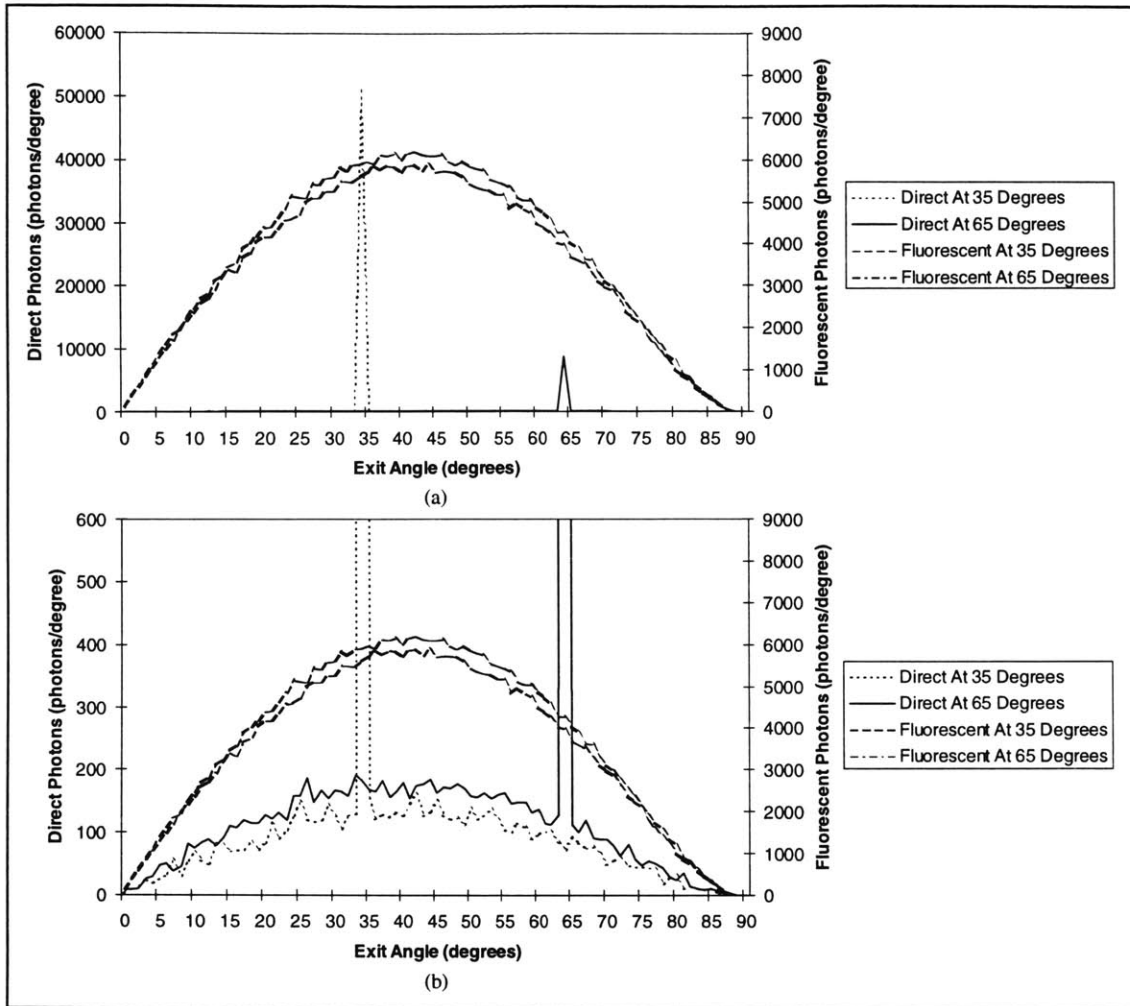


**Figure 28- (a) Angular Distribution of Direct and Fluorescent Photons for Two Input Angles (b) Scaled version of (a) (Diffuse Reflective Side Boundary; 1,000,000 Photons; Separated Emission/Excitation; Diameter = 1.0cm; Length = 1.0cm; Peak Absorption Coefficient =  $2\text{cm}^{-1}$ ; Initial Excitation=254nm)**

A person seeking to maximize fluorescence would maintain a wide field of view (high input angles) with a cladded material or a material with diffuse reflective sides. This would maximize the chance of non-absorbed photons exiting through the side boundary and increase the path length a photon must travel before exiting the output surface. A person seeking to minimize fluorescence would not be able to do so by adjusting the input angle. Nevertheless, he would choose a narrow field of view (low input angles) in order to maximize the number of photons transmitted directly without being absorbed. The magnitude of the fluorescence would not be significantly affected, however. A summary of these choices is presented in Table 14.

Parameter	Maximize Fluorescence	Minimize Fluorescence
High Input Angle	<b>X</b>	
Low Input Angle		<b>X</b>

**Table 14- Parameter Choice for Each Goal**



## 4.4 Diameter of Input

Spectral Characteristics	Boundary Effects	Input Angle	Diameter of Input	Length/Diameter Ratio	Detector Configuration
Separated	Air	$\theta_i < \theta_A$	Flooded $d_1/d_2 = 1$	$l/d > 1$	Coupled
Overlapping	Cladding	$\theta_i > \theta_A$	Beam $d_1/d_2 < 1$	$l/d = 1$	Uncoupled
	Diffuse Reflective		Spot $d_1/d_2 \ll 1$	$l/d < 1$	

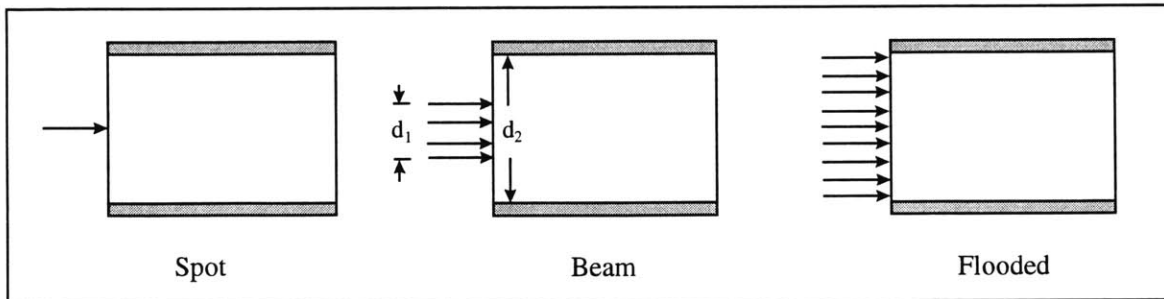


**Figure 29- Input Beam Diameter Configuration - The input diameter may range from an illumination of just a spot to fully flooding the aperture.**

The diameter of the source radiation beam can be adjusted from a spot all the way up to a size which floods the entrance aperture. The beam may be positioned at any location on the entrance surface. Three cases were considered, including a flooded input, a beam of half the radius of the material, and a centered spot. These cases are illustrated in Figure 29 and the input parameters for the simulation are shown in Table 15. The effect of input beam size on the fluorescence output is dependent on the length/diameter ( $l/d$ ) ratio of the material. This will be reflected in the analysis of the results.

Parameters	Input Diameter Test Cases		
	Flooded	Beam	Spot
Number of Photons	1M	1M	1M
Quantum Efficiency	80%	80%	80%
Excitation/Input	254nm	254nm	254nm
Material Index	n=1.5	n=1.5	n=1.5
Excitation/Emission Spectra	Separated	Separated	Separated
Entrance Surface Boundary	Air	Air	Air
Side Boundary	n=1.3	n=1.3	n=1.3
Exit Surface Boundary	Air	Air	Air
Input Angle	0 degrees	0 degrees	0 degrees
Input Beam Diameter	Flooded	Beam	Spot
Length	Varied	Varied	Varied
$\alpha l$	10	10	10
Material Diameter	1.0 cm	1.0 cm	1.0 cm
Detector Distance	0 cm	0 cm	0 cm
Detector Diameter	1.0 cm	1.0 cm	1.0 cm
Detector Index	n=1.0	n=1.0	n=1.0

**Table 15- Input Diameter Test Cases**

For a spot or beam input and a large  $l/d$  ratio, the number of fluorescent photons exiting the output surface is reduced, as shown Table 16 and Table 17. With a longer length of material, more photons exit the material through the side boundary. A flooded input increases the number of fluorescent photons exiting the output surface, compared to the spot and beam cases, as shown in Table 18.

Beam Input (Beam Diameter = 0.5cm)			
Length	0.2 cm	1.0 cm	5.0 cm
Reflected Off Front	40154	40106	40177
Absorbed; Not Re-radiated	192007	192301	192117
Exited Out Front; Direct	0	0	0
Exited Out Front; Fluorescent	95852	90382	81947
Exited Out Side; Direct	0	0	0
Exited Out Side; Fluorescent	574972	612227	629719
Exited Out Back; Direct	65	83	93
Exited Out Back; Fluorescent	96950	64901	55947
Trapped Inside (>50 Reflections)	0	0	0

**Table 16- Monte Carlo Test Results for Beam Input**

Spot Input At Center			
Length	0.2 cm	1.0 cm	5.0 cm
Reflected Off Front	40055	40054	39950
Absorbed; Not Re-radiated	191906	191668	192614
Exited Out Front; Direct	0	0	0
Exited Out Front; Fluorescent	97436	90879	81312
Exited Out Side; Direct	0	0	0
Exited Out Side; Fluorescent	574264	618666	634190
Exited Out Back; Direct	83	77	95
Exited Out Back; Fluorescent	96256	58654	51839
Trapped Inside (>50 Reflections)	0	2	0

**Table 17- Monte Carlo Test Results for Spot Input**

Flooded Input			
Length	0.2 cm	1.0 cm	5.0 cm
Reflected Off Front	40060	39569	40066
Absorbed; Not Re-radiated	192049	191743	192112
Exited Out Front; Direct	0	0	0
Exited Out Front; Fluorescent	95758	91537	86063
Exited Out Side; Direct	0	0	0
Exited Out Side; Fluorescent	527161	545013	559718
Exited Out Back; Direct	86	78	84
Exited Out Back; Fluorescent	93463	80483	70622
Trapped Inside (>50 Reflections)	51423	51577	51335

**Table 18- Monte Carlo Test Results for Flooded Input**

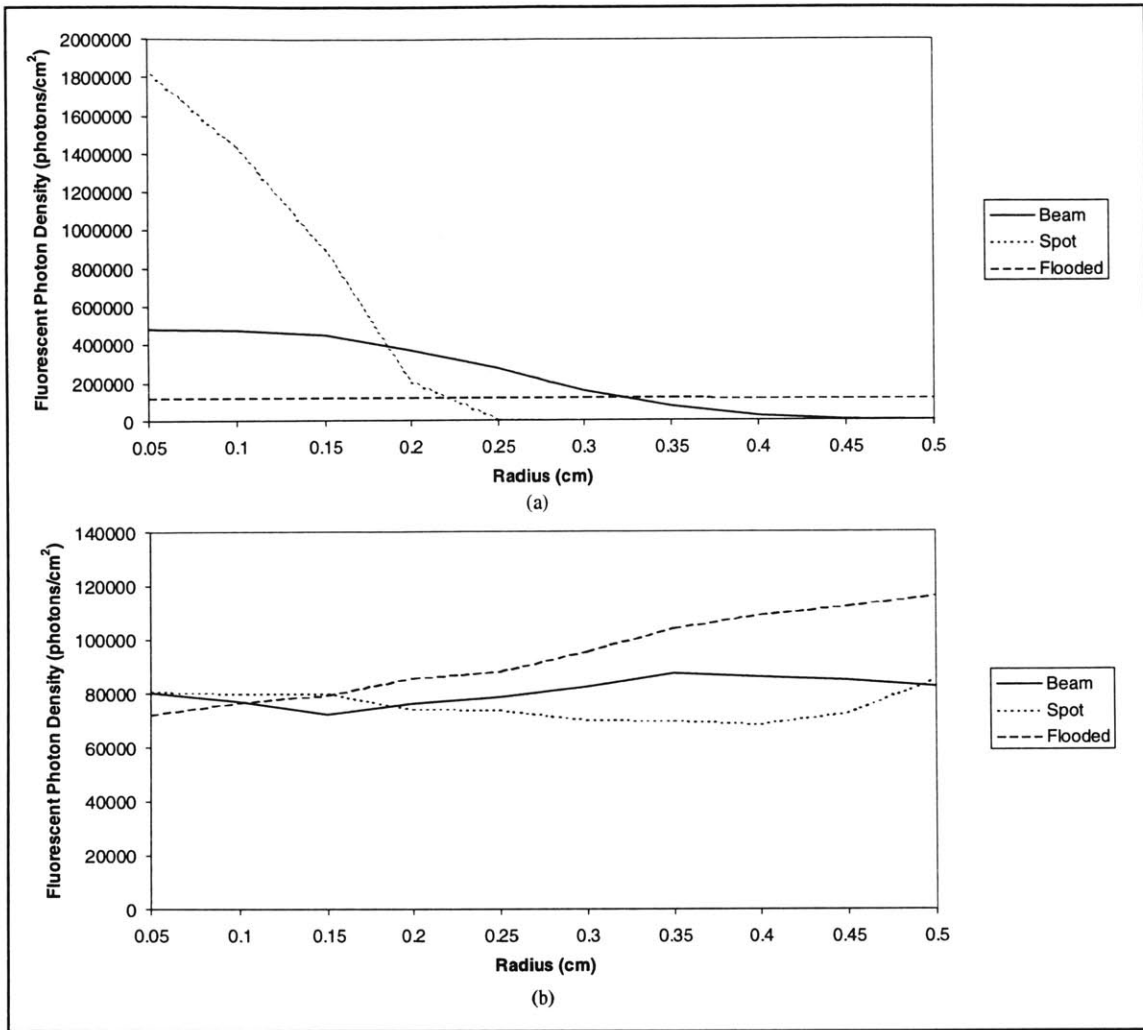


**Figure 30- Fluorescent Photon Spatial Distribution for Various Input Diameters (a) Length/Diameter Ratio = 0.2 (b) Length/Diameter Ratio = 1.0 (1,000,000 Photons; Separated Emission/Excitation; Diameter = 1.0cm; Absorption Coefficient-Length Product = 10; Initial Excitation=254 nm;  $n_i/n_c = 1.5/1.3$ )**

The effect of input diameter is a function of the material length/diameter ( $l/d$ ) ratio. For a small  $l/d$  ratio, the spatial distribution on the output surface is strongly dependent on the input beam size, as shown in Figure 30(a). On the other hand, for  $l/d=1$ , the spatial distribution is relatively independent of the input beam size. This effect can be seen in Figure 30(b).

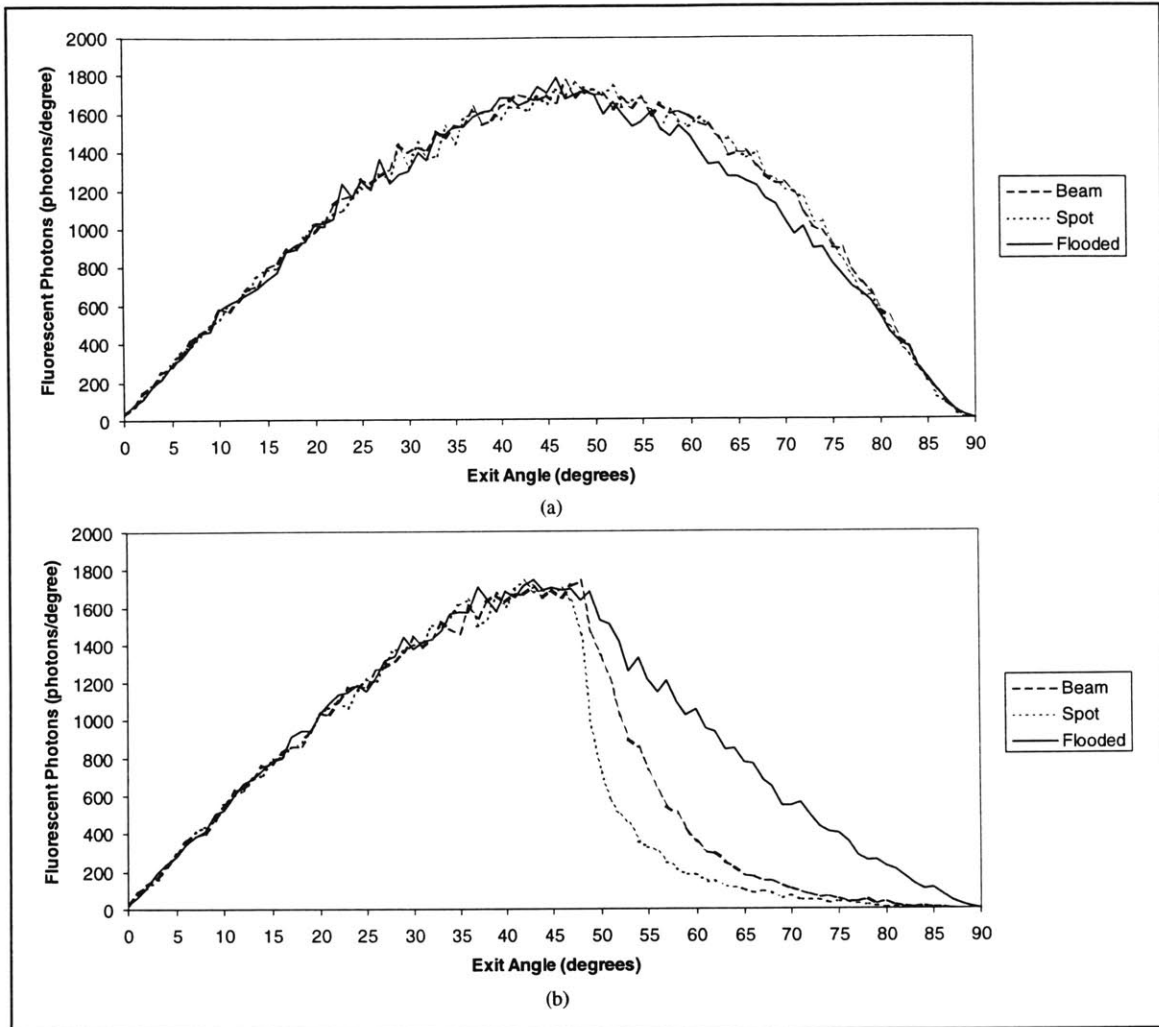


**Figure 31- Fluorescent Photon Angular Distribution for Various Input Diameters (a) Length/Diameter Ratio = 0.2 (b) Length/Diameter Ratio = 1.0 (1,000,000 Photons; Separated Emission/Excitation; Diameter = 1.0cm; Absorption Coefficient-Length Product = 10; Initial Excitation=254 nm;  $n_i/n_c = 1.5/1.3$ )**

The output angular distribution is relatively independent of input beam size for small  $l/d$  ratios. However, for  $l/d=1$ , the output angular distribution is a strong function of input beam size. The relative magnitude of fluorescent photons exiting the output surface is a weak function of input beam diameter. These dependencies are shown in Figure 31 above.

The input beam size is an important parameter in adjusting the spatial and angular distributions of fluorescent output. The impact on the magnitude of the fluorescence output is summarized in Table 19.

Parameter	Maximize Fluorescence	Minimize Fluorescence
Flooded Input	<b>X</b>	
Beam Input		<b>X</b>
Spot Input		

**Table 19- Parameter Choice for Each Goal**

## 4.5 Length/Diameter Ratio

Spectral Characteristics	Boundary Effects	Input Angle	Diameter of Input	Length/Diameter Ratio	Detector Configuration
Separated	Air	$\theta_i < \theta_A$	Flooded $d_1/d_2 = 1$	$l/d > 1$	Coupled
Overlapping	Cladding	$\theta_i > \theta_A$	Beam $d_1/d_2 < 1$	$l/d = 1$	Uncoupled
	Diffuse Reflective		Spot $d_1/d_2 \ll 1$	$l/d < 1$	

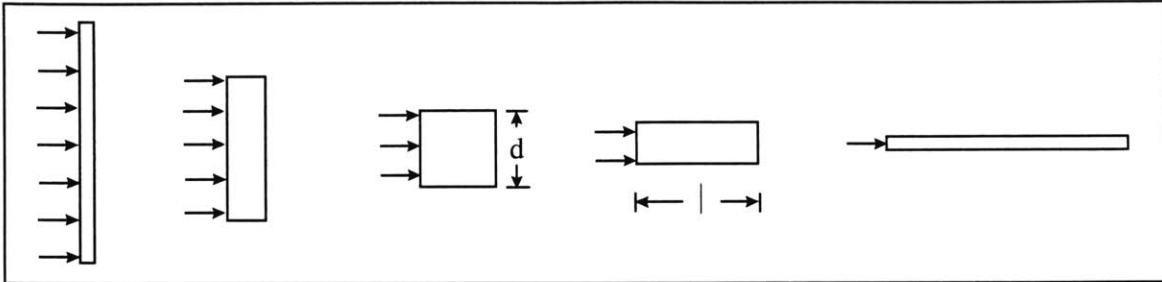


**Figure 32- Length/Diameter Ratio Configuration - The length/diameter ratio may range from a short, wide geometry to a long, narrow geometry.**

The user of the model can select the cylindrical dimensions of the material by specifying a length and diameter, as illustrated in Figure 32. Any geometric effect caused by changing these dimensions will be related to the ratio of length to diameter ( $l/d$ ), since the photons in the model are without dimension.

The  $l/d$  ratio affects both the magnitude of fluorescent photons exiting the output surface and the angular distribution of those photons. The overall effect is dependent on the boundary conditions of the material. Therefore, three cases are considered, as listed in Table 20.

Parameters	Length/Diameter Ratio Test Cases		
	Cladded	Air	Diffuse Reflective
Number of Photons	1M	1M	1M
Quantum Efficiency	80%	80%	80%
Excitation/Input	254nm	254nm	254nm
Material Index	n=1.5	n=1.5	n=1.5
Excitation/Emission Spectra	Separated	Separated	Separated
Entrance Surface Boundary	Air	Air	Air
Side Boundary	Cladded n=1.3	Air n=1.0	Diffuse Reflective
Exit Surface Boundary	Air	Air	Air
Input Angle	0 degrees	0 degrees	0 degrees
Input Beam Diameter	Flooded	Flooded	Flooded
Length	l=1.0 cm	l=1.0 cm	l=1.0 cm
$\alpha$ l	10	10	10
Material Diameter	Varied	Varied	Varied
Detector Distance	0 cm	0 cm	0 cm
Detector Diameter	1.0 cm	1.0 cm	1.0 cm
Detector Index	n=1.0	n=1.0	n=1.0

**Table 20- Length/Diameter Ratio Test Cases**

The effect of the  $l/d$  ratio on the magnitude of fluorescence output is shown in Figure 33. The effect is dependent on the side boundary condition of the material. The magnitude is strongly increased for a diffuse reflective boundary and a small  $l/d$ . The effect decreases as the  $l/d$  ratio increases, arguing for a shorter length when trying to maximize fluorescence.



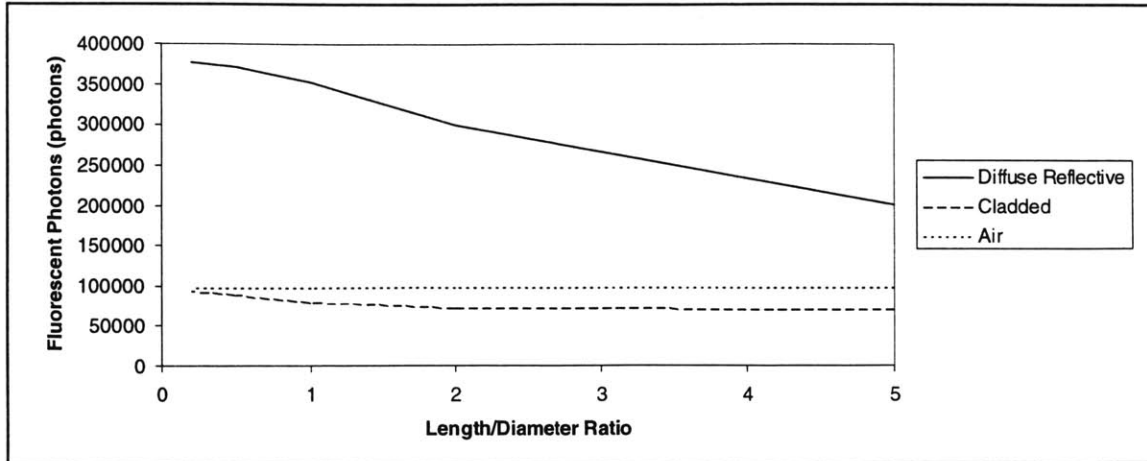


**Figure 33- Fluorescent Photons vs. Length/Diameter Ratio for Various Boundary Conditions (1,000,000 Photons; Separated Emission/Excitation; Diameter = 1.0cm; Absorption Coefficient-Length Product = 10; Initial Excitation=254nm;  $n_i/n_c = 1.5/1.3$ , for Cladded Case)**

The effects of  $l/d$  ratio on angular distribution for various boundaries can be seen in Figure 34. With an air boundary, the angular distribution is unaffected by the  $l/d$  ratio. A cladded boundary leads to a loss of photons at high angles, compared to a Lambertian distribution, due to an increased loss of photons out the side boundary. A diffuse reflective boundary causes a narrowing of the distribution for larger  $l/d$  ratios.

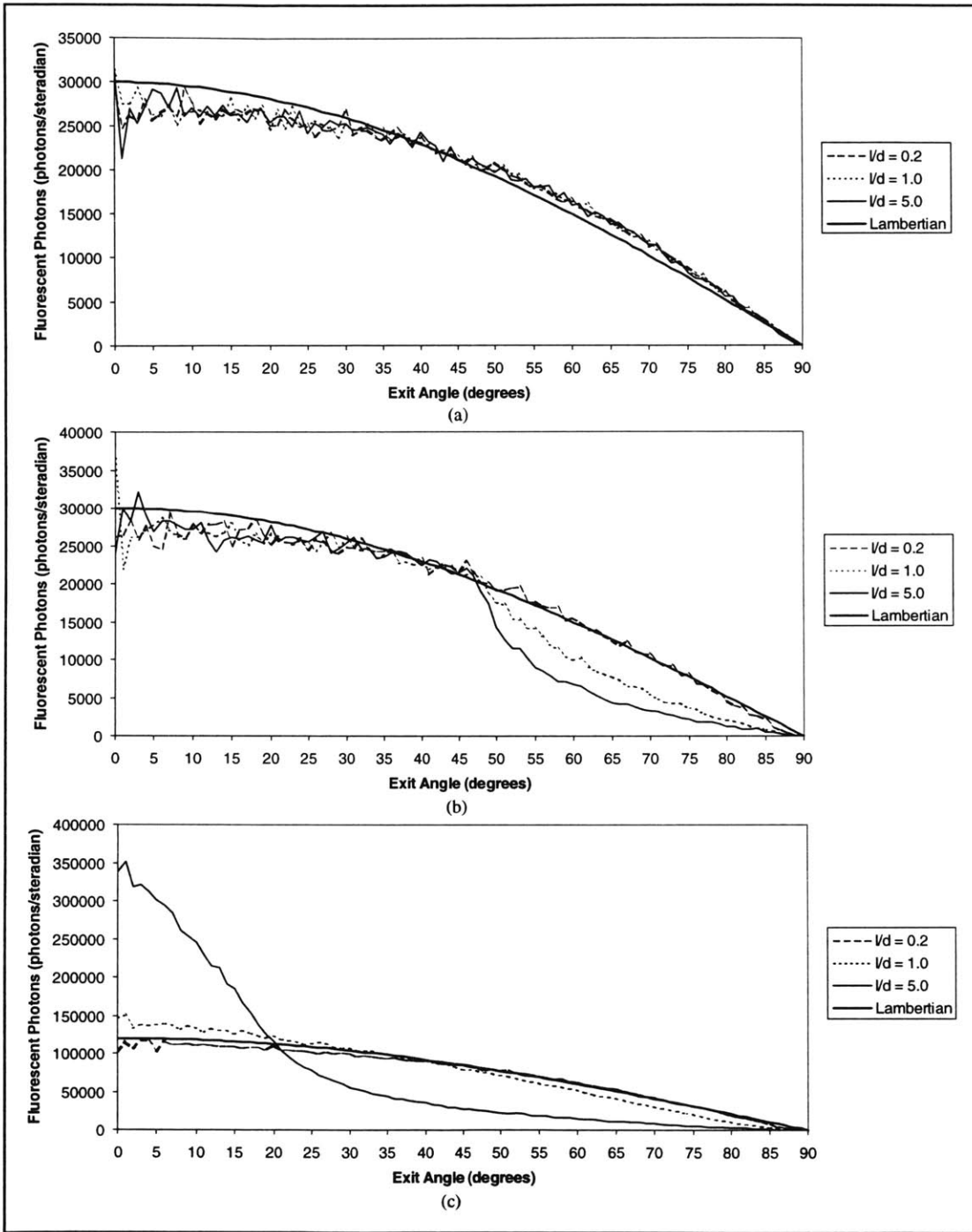


**Figure 34- Fluorescent Photon Angular Distributions for Various Length/Diameter Ratios (a) Air Boundary (b) Cladded Boundary (c) Diffuse Reflective Boundary (1,000,000 Photons; Separated Emission/Excitation; Diameter = 1.0cm; Absorption Coefficient-Length Product = 10; Initial Excitation=254 nm;  $n_i/n_c = 1.5/1.3$ , for Cladded Case)**

A person seeking to maximize the fluorescence exiting the output surface would choose a thin element with a larger diameter (small  $l/d$ ) and a diffuse reflective boundary. A person trying to reduce fluorescence would choose a thicker element and smaller diameter with a cladded side boundary. These choices are shown in Table 21.

Parameter	Maximize Fluorescence	Minimize Fluorescence
$l/d < 1$	<b>X</b>	
$l/d = 1$		
$l/d > 1$		<b>X</b>

**Table 21- Parameter Choice for Each Goal**

## 4.6 Detector Configuration

Spectral Characteristics	Boundary Effects	Input Angle	Diameter of Input	Length/Diameter Ratio	Detector Configuration
Separated	Air	$\theta_i < \theta_A$	Flooded $d_1/d_2 = 1$	$l/d > 1$	Coupled
Overlapping	Cladding	$\theta_i > \theta_A$	Beam $d_1/d_2 < 1$	$l/d = 1$	Uncoupled
	Diffuse Reflective		Spot $d_1/d_2 \ll 1$	$l/d < 1$	

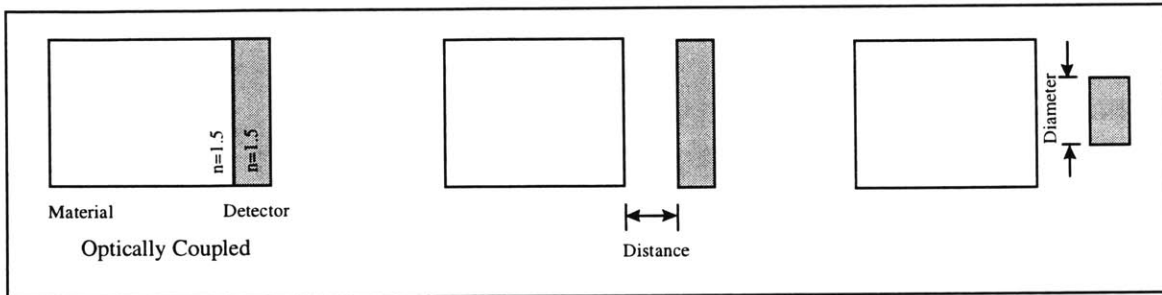


**Figure 35- Detector Configuration - The detector may be coupled or uncoupled. The detector's diameter and distance from the material may be adjusted as well.**

The detector may be coupled to the fluorescing material or remain uncoupled. In either case, the diameter of the detector may be sized as desired. When uncoupled, the distance between the output surface of the material and the detector can be adjusted in order to affect the number of fluorescent photons which are recorded by the detector. These possibilities are illustrated in Figure 35.

When the detector is placed at some nonzero distance from the output surface of the material, air fills the gap. The air boundary at the output surface allows photons inside the material to sometimes exit the material and sometimes reflect back into the material, depending on their angle of incidence with the boundary. If the detector was, instead, placed at zero distance, and furthermore was of the same index as the material, the detector would be considered “optically coupled” or “matched”. Photons incident upon

the boundary between the output surface and the detector would always pass through to the detector. Two cases, coupled and uncoupled, are considered in this section. The input parameters for these cases are summarized in Table 22.

Parameters	Detector Configuration Cases	
	Coupled	Uncoupled
Number of Photons	1M	1M
Quantum Efficiency	80%	80%
Excitation/Input	254nm	254nm
Material Index	n=1.5	n=1.5
Excitation/Emission Spectra	Separated	Separated
Entrance Surface Boundary	Air	Air
Side Boundary	n=1.3	n=1.3
Exit Surface Boundary	Air	Air
Input Angle	0 degrees	0 degrees
Input Beam Diameter	Flooded	Flooded
Length	Varied	Varied
$\alpha$	Varied	Varied
Material Diameter	1.0 cm	1.0 cm
Detector Distance	0 cm	0 cm
Detector Diameter	1.0 cm	1.0 cm
Detector Index	n=1.5	n=1.0

**Table 22- Detector Configuration Cases**

The effect of optically coupling the detector to the fluorescing material is dramatic, as shown in Table 23 and Table 24.

Optically Coupled Detector (Matched Index = 1.5)					
Length	0.2 cm	0.5 cm	1.0 cm	2.0 cm	5.0 cm
Reflected Off Front	39806	40072	39821	40310	40325
Absorbed; Not Re-radiated	165625	190826	192256	192156	191517
Exited Out Front; Direct	0	0	0	0	0
Exited Out Front; Fluorescent	75898	86549	86646	86475	86796
Exited Out Side; Direct	0	0	0	0	0
Exited Out Side; Fluorescent	272143	465916	538575	551844	555025
Exited Out Back; Direct	129571	6506	83	43	51
Exited Out Back; Fluorescent	316515	208760	139949	124021	113974
Trapped Inside (>50 Reflections)	442	1371	2670	5151	12312

**Table 23- Monte Carlo Test Results for Optically Coupled Detector**

Uncoupled Detector (Air Index = 1.0)					
Length	0.2 cm	0.5 cm	1.0 cm	2.0 cm	5.0 cm
Reflected Off Front	39910	39803	39831	40092	39874
Absorbed; Not Re-radiated	166791	190806	192995	192189	192877
Exited Out Front; Direct	720	0	0	0	0
Exited Out Front; Fluorescent	82413	91880	91487	91333	91077
Exited Out Side; Direct	0	0	0	0	0
Exited Out Side; Fluorescent	459074	532153	544626	552520	554248
Exited Out Back; Direct	124700	6161	85	71	51
Exited Out Back; Fluorescent	81826	88253	79667	72357	70070
Trapped Inside (>50 Reflections)	44566	50944	51309	51438	51803

**Table 24- Monte Carlo Test Results for Uncoupled Detector**

In an optically coupled setup, the number of fluorescent photons increases significantly, as all photons which reach the output surface boundary escape the material. Figure 36 shows graphically the increase in fluorescence magnitude for a coupled detector. It is apparent that one would choose a shorter length material to maximize fluorescence, as the effect of coupling decreases for longer lengths.

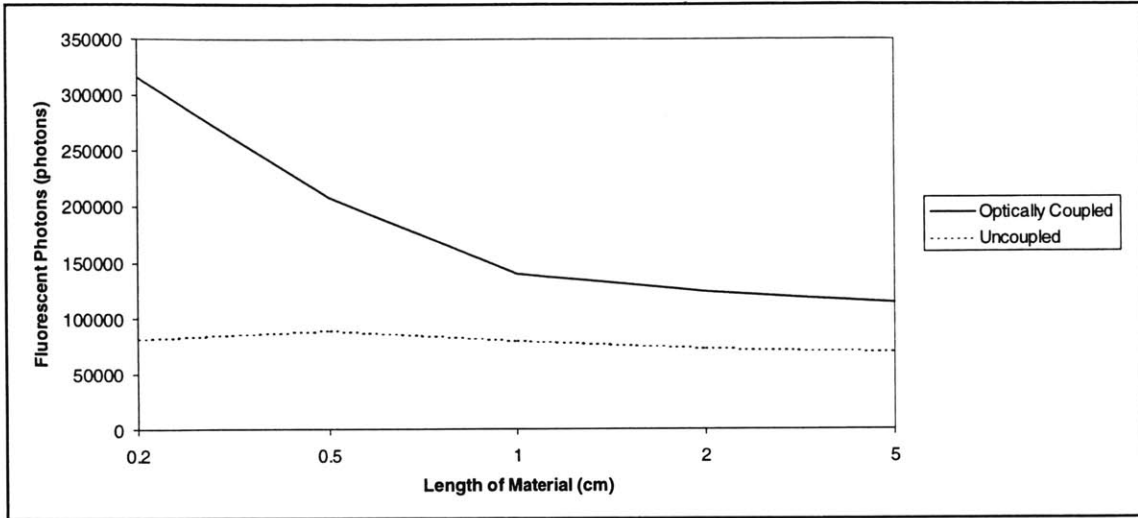


**Figure 36- Fluorescent Photons vs. Material Length for Optically Coupled and Uncoupled Detectors (1,000,000 Photons; Cladded Boundary; Separated Emission/Excitation; Diameter = 1.0cm; Peak Absorption Coefficient =  $10\text{cm}^{-1}$ ; Initial Excitation=254nm;  $n_i/n_c = 1.5/1.3$ )**

The reason for the dramatic increase in fluorescence for shorter lengths can be seen in Figure 37. Fluorescent photons originating in the interior of the material may be emitted in any direction. For shorter lengths, a high number of photons aimed towards the entrance surface will be reflected off the inside of that surface. Those photons will end up exiting the output surface at high angles. Specifically, the angles are those which are greater than the critical angle for the material and entrance surface boundary, since angles greater than the critical angle for that surface get reflected and end up exiting the output surface. The increased number of higher angled photons is seen Figure 37(b).

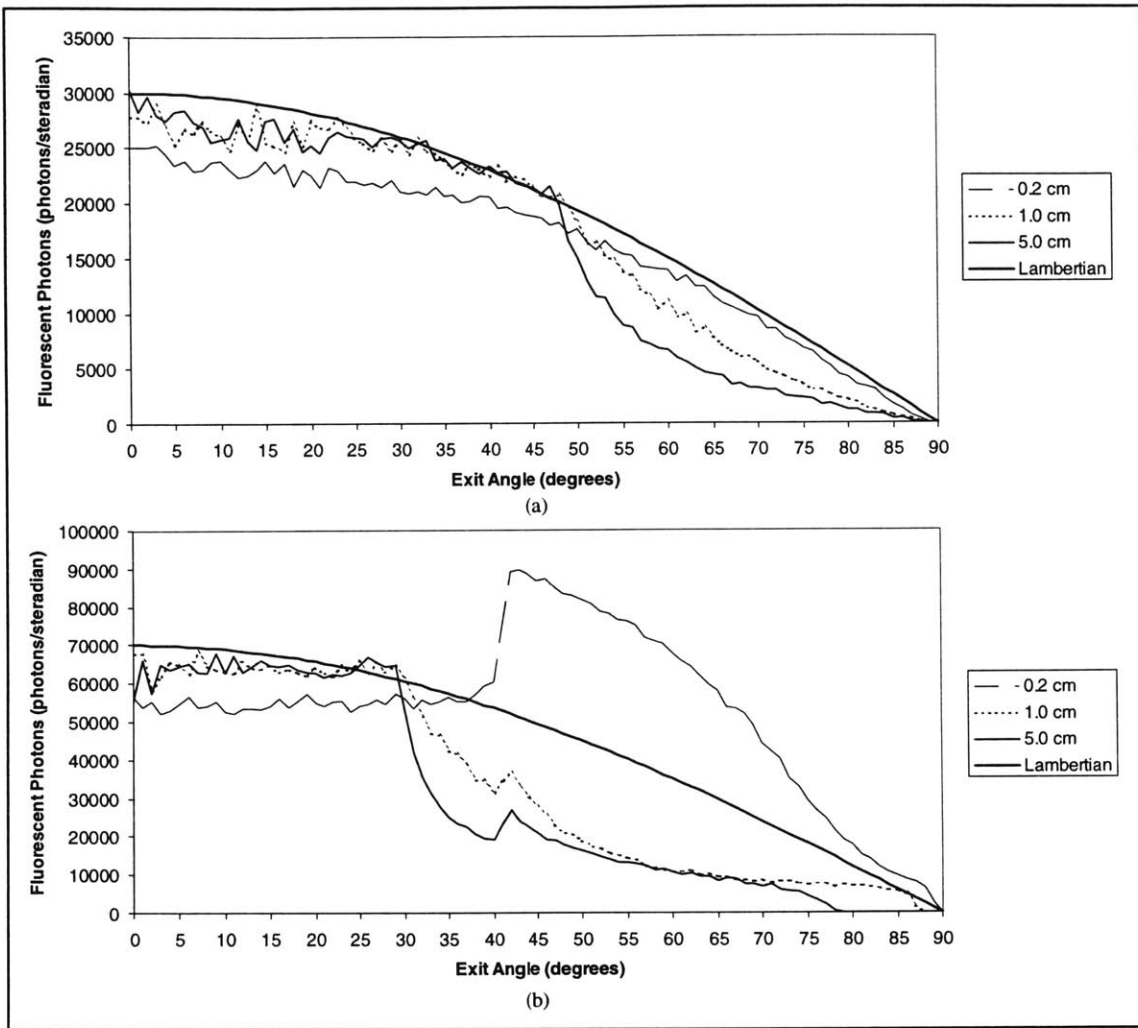


**Figure 37- Fluorescent Photon Angular Distribution for Various Lengths (a) Uncoupled (b) Optically Coupled (1,000,000 Photons; Cladded Boundary; Separated Emission/Excitation; Diameter = 1.0cm; Peak Absorption Coefficient =  $10\text{cm}^{-1}$ ; Initial Excitation=254nm;  $n_i/n_c=1.5/1.3$ )**

In an uncoupled setup, the size of the air gap is not significant in changing the fluorescence output. The gap could be used to one's advantage, however. For example, photons exiting the output surface at high angles could be caused to miss the detector if the detector had a small enough diameter and was placed far enough away.



Fluorescence collection is enhanced by optically coupling the detector to the material. Having an air gap, on the other hand, minimizes the impact of fluorescence in the optical system. Therefore, one would make the choices shown in Table 25.

Parameter	Maximize Fluorescence	Minimize Fluorescence
Optically Coupled Detector	<b>X</b>	
Uncoupled/Air Gap		<b>X</b>

**Table 25- Parameter Choice for Each Goal**

## 5.0 Design Considerations

The previous section discussed some general rules for what to expect when adjustments to input parameters are made. This section will focus on the choices one would make to achieve specific objectives. Two possible design objectives will be considered. The goal for both objectives is to achieve the greatest possible signal to noise ratio for optimum performance.

The first design objective will be to create a wavelength shifter which has an excitation peak at the wavelength matching the source of interest. The wavelength shifter will seek to maximize the fluorescence resulting from the in-band signal and to yield the fluorescence in a band of wavelengths significantly longer than the source. Such a configuration can be used to take advantage of desirable detector technologies.

The second design objective will be to create a spectral filter which maximizes the signal of interest, but seeks to minimize fluorescence which results from out-of-band, background sources. Detection of the in-band signal requires that competing background sources be sufficiently (and often significantly) rejected. Materials which provide this desirable absorption also have a “side effect” of generating fluorescence. An effort will be made to minimize the impact of fluorescence on the overall optical system performance.

For each case, choices for parameters will be based on design constraints and by comparisons of parameters considered in the previous section. The major parameter choices can be categorized into physical, boundary, detector interface, and input beam parameters. A summary of the choices which will be made for each objective are presented in Table 26.

Category	Parameter	Wavelength Shifter	Direct Detector
Material	Fluorescent Quantum Yield	High	Low
Physical	Length/Diameter Ratio	Small	Large
Boundaries	Input Surface	AR at Excitation Peak; Reflective at Emission Wavelengths	AR at Direct Wavelength
	Side Wall Configuration	Diffuse Reflective	Cladding
Detector Interface	Detector Coupling	Yes	No
	Detector Distance	0 cm	>0 cm
	Detector Diameter	Same as Material	Same as Input Beam
Input Beam	Input Beam Diameter	Flooded	Beam

**Table 26- Parameter Choices for Each Goal**

The general approach taken to choose parameters in a real life situation is illustrated in Figure 38 below.

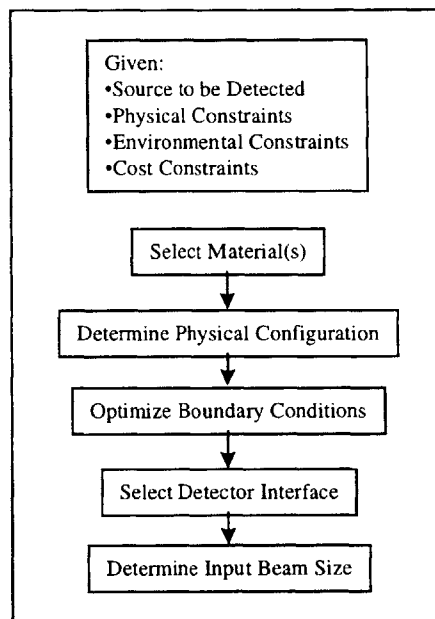


**Figure 38- Parameter Selection Procedure**

## 5.1 Maximizing Fluorescence – Wavelength Shifter

*Design a wavelength shifter which has an excitation peak at 254nm and emission at 500nm.*

The material chosen for the wavelength shifting design problem should have many absorbers, so that a maximum amount of conversion from incident wavelength to fluorescence will occur. Therefore, one would choose a crystal or doped glass with a high doping concentration. It is also important to have the shortest possible length to allow a maximum amount of fluorescence to be transmitted. Often, practical limits require that one choose a maximum concentration of material and then determine the appropriate length. The path length,  $l$ , will be chosen such that  $e^{-\alpha l}$  is less than 0.1%.

The treatment choice for the side boundary will have a significant affect on the fluorescence output magnitude, as discussed in Section 4.2. As recommended in Table 12, the side boundary will be appropriately coated to make it diffuse reflective.

To eliminate loss at the exit surface, the detector will be optically coupled to the fluorescing material. The benefit of this configuration are shown Figure 37. The detector diameter will be identical to the fluorescing element, since the fluorescence output is spread across the exit surface. The input surface will be treated such that it is antireflective at the excitation wavelength to maximize input at the wavelength of interest, and reflective at the emission wavelengths to minimize loss of fluorescence back out the entrance surface. The result will be that 100% of the fluorescent photons will be collected, and the number will be proportional to the fluorescent quantum yield.

## 5.2 Minimizing Fluorescence – Direct Detection

*Design a spectral filter to detect at 254nm and reject out-of-band sources.*

To optimize the design for direct detection, a material with a low concentration and longer length combination should be chosen to meet the specified transmission requirement,  $\alpha l$ . The longer length will allow for self absorption in the bulk of the material (Section 4.1), assuming the material has overlapping excitation and emission spectra. The longer length will also permit a larger number of fluorescent photons to escape out of the side.

The side boundary will be surrounded with a cladding whose index of refraction comes as close to matching that of the fluorescing material within the constraints of the input acceptance angle. The more closely the indices are matched, the more easily fluorescent photons will transmit through the side boundary. However, the acceptance angle is reduced by the close matching, as indicated in Section 4.3.

An air gap will be placed between the fluorescing element and the detector to increase fluorescence loss at the output surface, as indicated in Section 4.6. The detector diameter will be smaller than the diameter of the fluorescing element so that high angled fluorescence and fluorescence near the outer radius of the output surface may avoid the detector. The detector diameter could be matched in size to the input beam diameter or the spatial distribution at the output surface. An antireflective coating at the in-band wavelength will be applied to the front surface to maximize the direct signal.

## 6.0 Conclusion/Recommendations

A Monte Carlo simulation model which predicts fluorescence behavior in a transmission geometry has been demonstrated. An optical designer could use this model to predict intensity, angular distribution, and spatial distribution of both directly transmitted radiation and fluorescence emitted from within a material. The designer can modify the material properties and conditions on the optical system to see the effect of possible design tradeoffs.

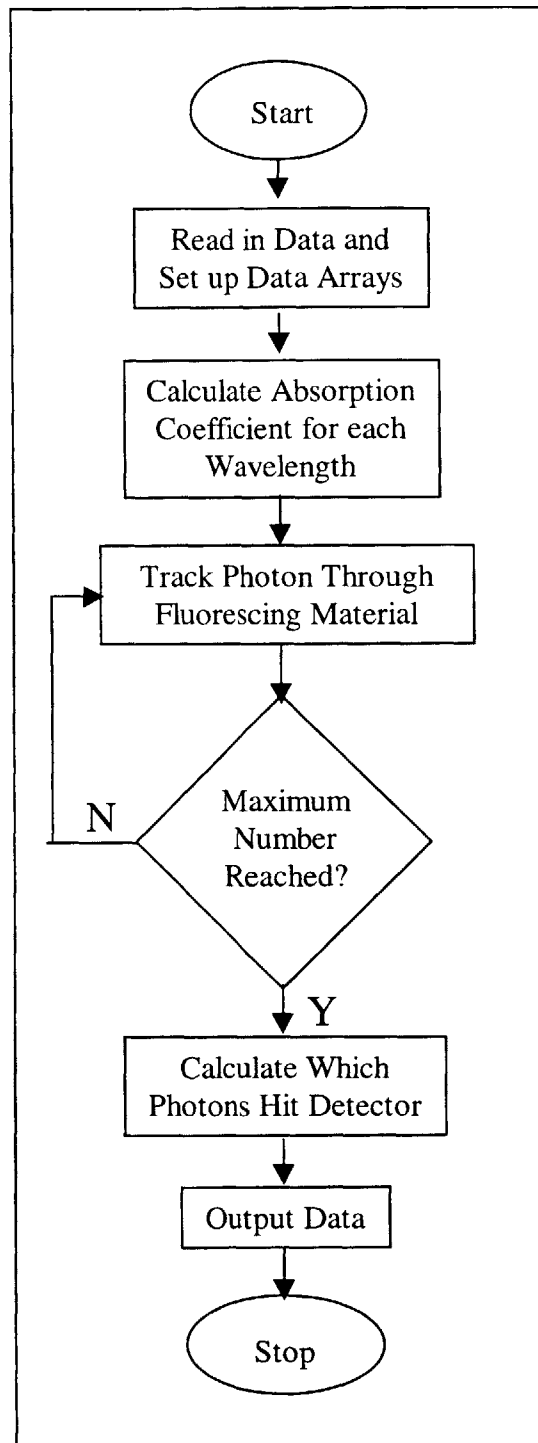
With due consideration for input and output parameters, this model could be incorporated into larger optical design or ray-trace packages. The larger ray-trace program would consider multiple elements with more parameters and would predict which photons reached the focal plane. To facilitate incorporation, the parts of the model which control the input characteristics of a photon would need to be changed from generating their own photons to accepting photon characteristics from the larger ray-trace program. Also, the output of the model would need to be in a form that the larger program could accept.

The model, as a stand alone design tool or part of a larger program, could be improved upon. Scattering could be added in a modular way. The probability of a bulk scattering event can be determined in a manner very similar to that of an absorbing event. Surface scattering could be a probabilistic event, resulting in a hybrid boundary of part Fresnel reflector, part diffuse reflector. Another improvement would be to allow for other geometries of fluorescing elements, particularly shapes which improve the fluorescence rejection or enhancement or lens shapes which would affect the overall properties of the

optical system. The detector portion of the model could be modified to mimic a spatial detector, providing results in terms of which pixels detect photons.

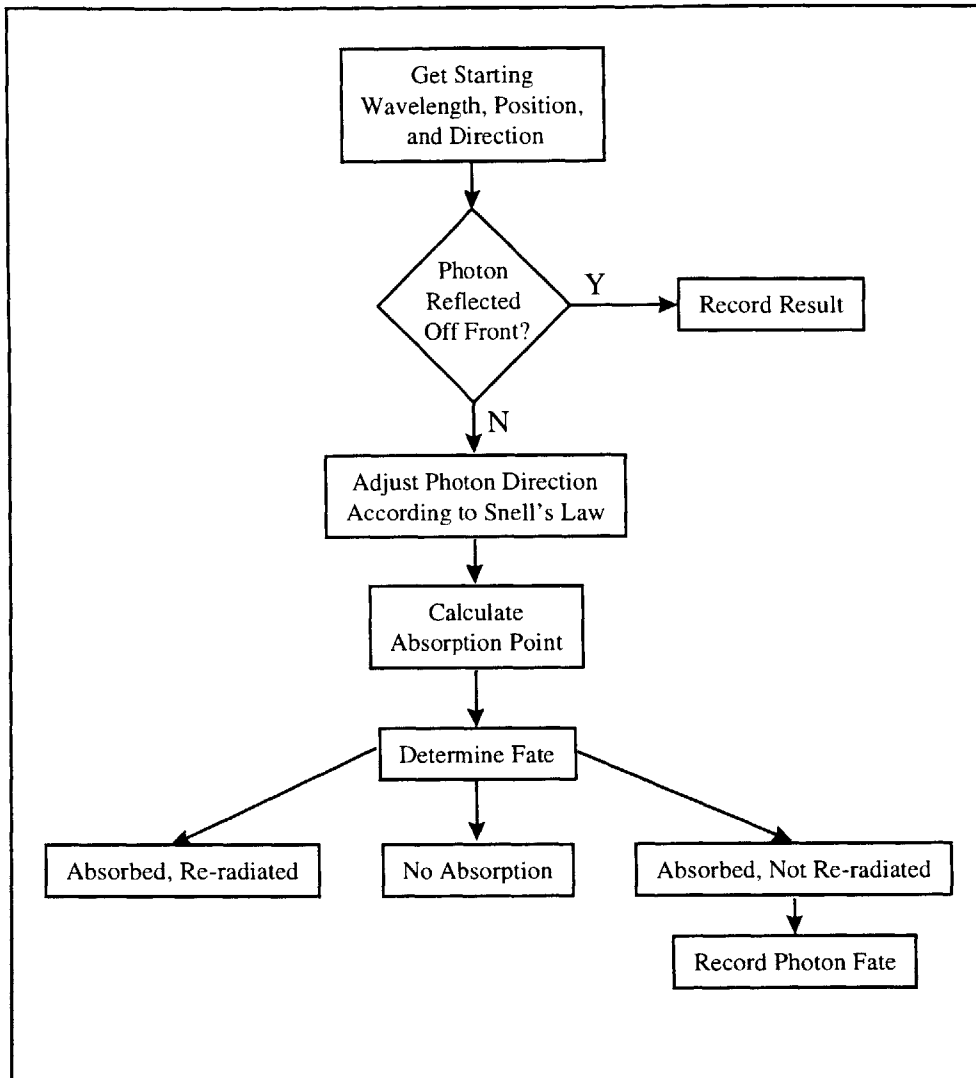
The model has the potential to work in a reverse direction, as well. For example, the model could be extended for use in biological systems to determine the individual fluorescing pigments by changing parameters in the model until the fluorescent output matched. An iterative process might allow one to decompose complex spectra. Furthermore, the complex spectra of these systems could be incorporated into the model to determine sensitivity to concentration and excitation spectra, resulting in optimized experiments.

## Appendix A – Flow Chart of Monte Carlo Simulation

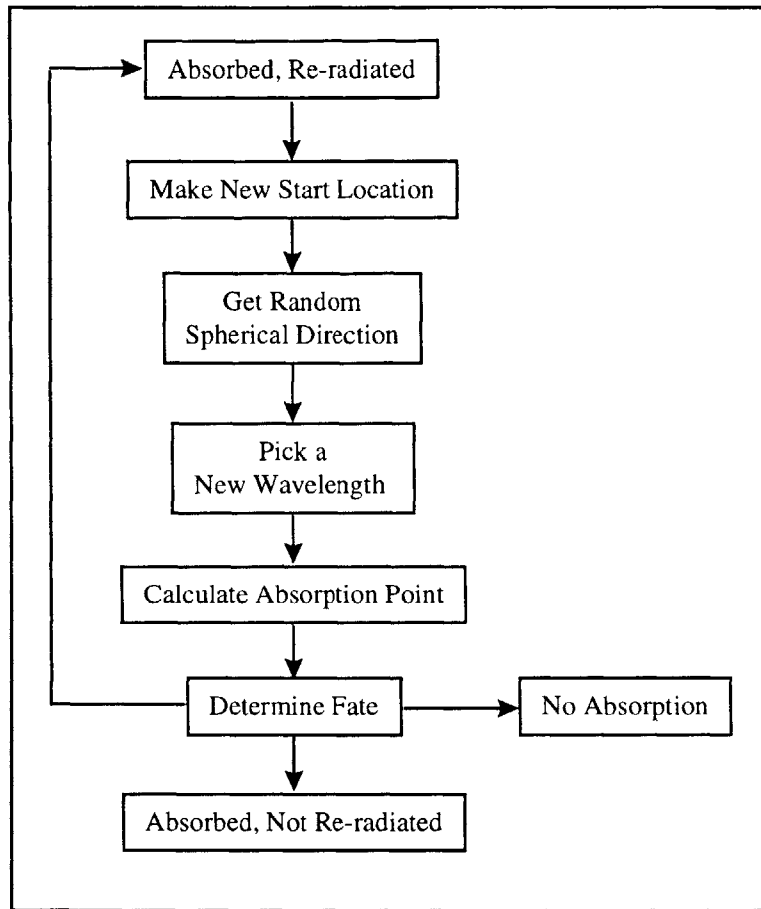


Top Level Simulation Process

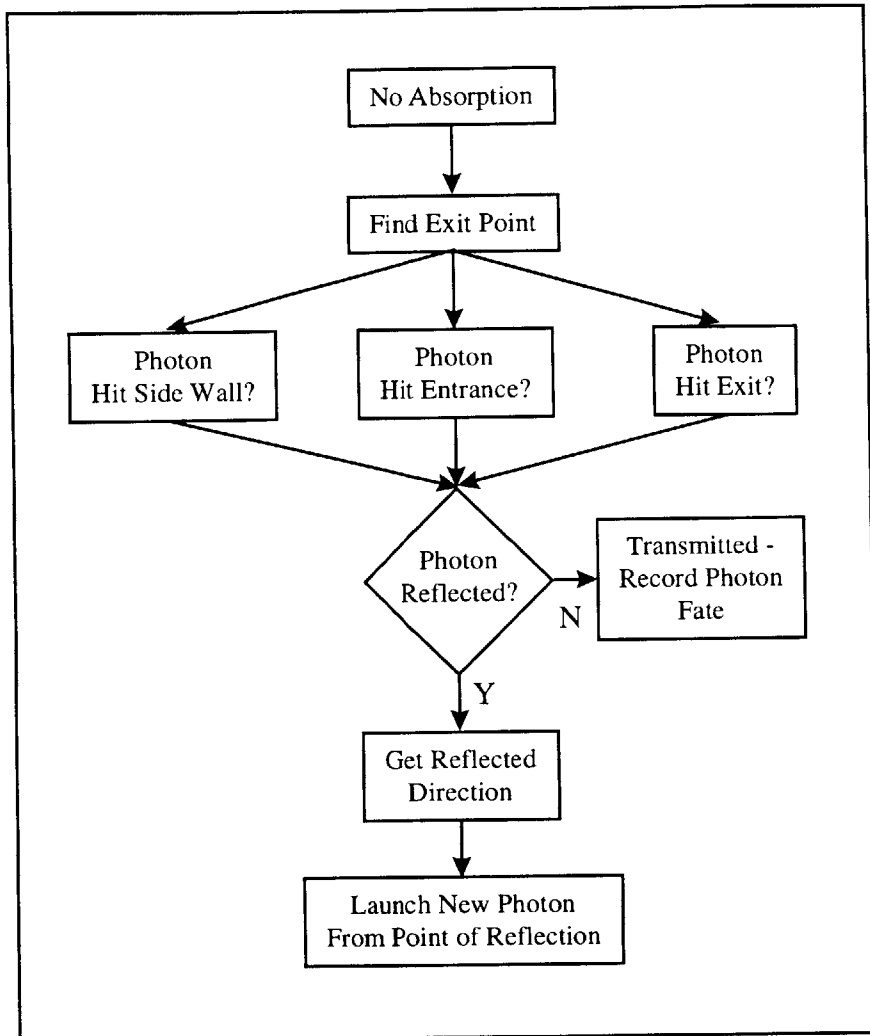




Tracking Photons Through Material



Absorbed and Re-radiated



No Absorption

## References

- 
- <sup>1</sup> McKee, David J., ed. Tropospheric Ozone: Human Health and Agricultural Impacts. Lewis: Boca Raton, 1994.
  - <sup>2</sup> Preisendorfer, R. W. Hydrologic Optics. Joint Tsunami Research Effort. Honolulu, Hawaii. 1976.
  - <sup>3</sup> Frenkel, A., et al. "Photon-noise-limited operation of intensified CCD cameras". Applied Optics. 1 August, 1997.
  - <sup>4</sup> Lacaíta, A. et al. "Single-photon detection beyond 1 $\mu$ m: performance of commercially available InGaAs/InP detectors". Applied Optics. 1 June, 1996.
  - <sup>5</sup> Joseph, Charles L. "UV Image Sensors and Associated Technologies". Experimental Astronomy. Vol. 6: 97-127, 1995.
  - <sup>6</sup> Csorba, Illes P. Image Tubes. Howard W. Sams & Co., Inc.
  - <sup>7</sup> Rzeghi, M. and A. Rogalski. "Semiconductor ultraviolet detectors". Journal of Applied Physics. 15 May, 1996.
  - <sup>8</sup> Higgins, Thomas V. "How Optical Materials Respond to Light". Laser Focus World. July, 1994.
  - <sup>9</sup> Jenkins, Francis A. and Harvey E. White. "Chapter 22- Absorption and Scattering". Fundamentals of Optics. 1976.
  - <sup>10</sup> Zink, Jeffrey. "Squeezing Light Out of Crystals: Triboluminescence". Dept. of Chemistry, University of California, Los Angeles, California 90024. Springer-Verlag 1981.
  - <sup>11</sup> Sweeting, Linda, et al. "Crystal Structure and Triboluminescence 2.9-Anthracenecarboxylic Acid and Its Esters". Chem. Mater. Vol. 9, No. 5, 1997.
  - <sup>12</sup> Saleh, B. E. A. and M. C. Teich. Fundamentals of Photonics. John Wiley & Sons, Inc.: New York, 1991.
  - <sup>13</sup> Vrij, D. R. ed. Luminescence of Solids. New York: Plenum, 1998.
  - <sup>14</sup> Scott, Herman. "Plant Fluorescence Sensor". Aerodyne Research, Inc.
  - <sup>15</sup> Henkel, Stephanie. "Synchronous Fluorescence Spectrometry Could Make Needle Sticks Obsolete". Sensors. August 1996.
  - <sup>16</sup> Abrams, Susan B. "Fluorescent Markers: GFP Joins the Common Dyes". Biophotonics International. Mar/Apr 1998.
  - <sup>17</sup> Doubilet, David. "A New Light in the Sea". National Geographic.
  - <sup>18</sup> Raimondi, Valentina, et al. "Fluorescence lidar monitoring of historic buildings". Applied Optics. 20 February 1998.
  - <sup>19</sup> Burlamacchi, Pio, et al. "Performance evaluation of UV sources for lidar fluorosensing of oil films". Applied Optics. 1 January 1983.
  - <sup>20</sup> Garifo, Luciano. "Optical systems monitor atmospheric pollutants". Laser Focus World. April, 1997.
  - <sup>21</sup> Duclos, Steven J. "Scintillator Phosphors for Medical Imaging". The Electrochemical Society Interface. Summer 1998.
  - <sup>22</sup> Srivastava, Alok M. and Timothy Sommerer. "Fluorescent Lamp Phosphors". Interface. Summer 1998.

- 
- <sup>23</sup> Fux, Eran and Charles Mazel. “Unmixing coral fluorescence emission spectra and predicting new spectra under different excitation conditions”. Applied Optics. 20 January 1999.
- <sup>24</sup> Sumita Optical Glass. 4-7-25 Harigaya, Urawa, Saitama, 338-8565 Japan.  
[Http://www1.sphere.ne.jp/sumita/](http://www1.sphere.ne.jp/sumita/)
- <sup>25</sup> EG&G Ortec. “Instrumentation for Fluorescence Lifetime Spectrometry”. Application notes.
- <sup>26</sup> Computational Science Education Project (CSEP). Introduction To Monte Carlo Methods. 1995. (WWW source).
- <sup>27</sup> Frieden, B. Roy. Probability, Statistical Optics, and Data Testing. Springer-Verlag: New York, 1984.
- <sup>28</sup> Sassaroli, Angelo, et al. “Monte Carlo procedure for investigating light propagation and imaging of highly scattering media”. Applied Optics. Vol. 37, No. 31, 1 November 1998.
- <sup>29</sup> Prahl, S. A., et al. “A Monte Carlo Model of Light Propagation in Tissue”. SPIE Institute Series. Vol. IS 5 (1989).
- <sup>30</sup> Hecht, Eugene. Optics. 3<sup>rd</sup> ed. Addison-Wesley: New York, 1998.